Naval Surface Warfare Center
Carderock Division
West Bethesda, MD 20817-5700

NSWCCD-65-TR–2004/08 March 2004

Survivability, Structures, and Materials Division

Technical Report

Seaway Load Prediction Algorithms for High-Speed Hull Forms

by

Jerome P. Sikora and Nathan B. Klontz

NSWCCD-65-TR–2004/08 Seaway Load Prediction Algorithms for High-Speed Hull Forms

DEPARTMENT OF THE NAVY

NAVAL SURFACE WARFARE CENTER, CARDEROCK DIVISION
9500 MACARTHUR BOULEVARD
WEST BETHESDA MD 20817-5700

9110
Ser 65-51
29 Mar 04

From: Commander, Naval Surface Warfare Center, Carderock Division
To: Chief of Naval Research (ONR 334)

Subj: SEAWAY LOAD PREDICTIONS FOR HIGH-SPEED HULL FORMS

Ref: (a) Office of Naval Research Work Request WX40035/AA

Encl: (1) NSWCCD-65-TR–2004/08, *Seaway Load Prediction Algorithms for High-Speed Hull Forms*

1. Reference (a) requested the Naval Surface Warfare Center, Carderock Division (NSWCCD) to develop seaway load prediction algorithms for high-speed hull forms. Enclosure (1) documents the generation of several seaway load prediction algorithms for catamarans, trimarans, and surface effect ships based on available model and full-scale test data. These algorithms are intended for use as quick predictions of seaway loads during ship feasibility and concept design studies. As the ship design progresses and is refined, more accurate but time consuming computational analyses and model tests are appropriate.

2. Comments or questions may be referred to Mr. Nathan B. Klontz, Code 651; telephone (301) 227-4199; e-mail, KlontzNB@nswccd.navy.mil.

E.A. RASMUSSEN
By direction

Subj: SEAWAY LOAD PREDICTIONS FOR HIGH-SPEED HULL FORMS

Copy to:

COMNAVSEASYSCOM WASHINGTON DC
[SEA 05D1, SEA 05H, SEA 05P1]

CNR ARLINGTON VA [ONR 334 (Barsoum, Gagorik, Potter)]

DTIC FORT BELVOIR VA

NAVSURFWARCEN CARDEROCKDIV
BETHESDA MD [Codes 011, 2420 (Kennel), 3442 (TIC), 65, 651, 651 (Klontz (10 copies)), 652, 653, 654, 655]

Naval Surface Warfare Center
Carderock Division
West Bethesda, MD 20817-5700

NSWCCD-65-TR–2004/08 March 2004

Survivability, Structures, and Materials Department

Technical Report

Seaway Load Prediction Algorithms for High-Speed Hull Forms

by

Jerome P. Sikora and Nathan B. Klontz

Enclosure (1)

REPORT DOCUMENTATION PAGE

Form Approved OMB No. 0704-0188

1. REPORT DATE *(DD-MM-YYYY)*	2. REPORT TYPE	3. DATES COVERED *(From - To)*
1-Mar-2004	Final	-

4. TITLE AND SUBTITLE

Seaway Load Prediction Algorithms for High-Speed Hull Forms

5a. CONTRACT NUMBER
ONR WX40035/AA

5b. GRANT NUMBER

5c. PROGRAM ELEMENT NUMBER

6. AUTHOR(S)

Jerome P. Sikora and Nathan B. Klontz

5d. PROJECT NUMBER

5e. TASK NUMBER

5f. WORK UNIT NUMBER

7. PERFORMING ORGANIZATION NAME(S) AND ADDRESS(ES) AND ADDRESS(ES)

Naval Surface Warfare Center
Carderock Division
9500 Macarthur Boulevard
West Bethesda, MD 20817-5700

8. PERFORMING ORGANIZATION REPORT NUMBER

NSWCCD-65-TR-2004/08

9. SPONSORING / MONITORING AGENCY NAME(S) AND ADDRESS(ES)

Attn ONR 334
Chief of Naval Research
Ballston Centre Tower One
800 North Quincy Street
Arlington, VA 22217-5660

10. SPONSOR/MONITOR'S ACRONYM(S)

11. SPONSOR/MONITOR'S REPORT NUMBER(S)

12. DISTRIBUTION / AVAILABILITY STATEMENT

Approved for public release; distribution is unlimited.

13. SUPPLEMENTARY NOTES

14. ABSTRACT

This report documents the generation of several seaway load prediction algorithms for catamarans, trimarans, and surface effect ships based on available model and full-scale test data. These algorithms are intended for use as quick predictions of seaway loads during ship feasibility and concept design studies. Froude scaling laws are used for geometrically different ships for each ship and load type using first principles and empirically derived studies. Simple seaway load prediction algorithms are then developed and expressed as functions of ship displacement and various key ship particulars. These global load algorithms are quickly computed, making them suitable for preliminary or concept design studies. In some cases, algorithms were developed from a minimum amount of data, and it is anticipated that, as more data is gathered in the future, these algorithms will be further refined. As the ship design progresses and is refined, more accurate but time consuming computational analyses and model tests are appropriate. For completeness, previously developed algorithms for small waterplane area twin hull ships (SWATH) are included in the appendix.

15. SUBJECT TERMS

ship structures, seaway loads, catamarans, surface effects ships, trimarans

16. SECURITY CLASSIFICATION OF:			17. LIMITATION OF ABSTRACT	18. NUMBER OF PAGES	19a. NAME OF RESPONSIBLE PERSON
a. REPORT	b. ABSTRACT	c. THIS PAGE			Mr. Nathan B. Klontz
UNCLASSIFIED	UNCLASSIFIED	UNCLASSIFIED	SAR	42	19b. TELEPHONE NUMBER *(include area code)* (301)-227-4199

Contents

Figures

Page

Tables

Page

Administrative Information

This work described in this report was performed by the Structures and Composites Divsion (Code 65) of the Survivability, Structures, and Materials Department of the Naval Surface Warfare Center, Carderock Division (NSWCCD) during 2003. The work was sponsored by the In-house Applied Research program and was funded under the Office of Naval Research's (ONR) Work Request WX40035/AA.

Acknowledgements

The author's would like to acknowledge Mr. James Rodd (6510) for his support in developing the scaling laws for the seaway loads for catamarans and Mr. William Richardson (6540) for his support in developing lifetime loads for surface effect ships.

Introduction

The Navy has shown an interest in high-speed ships, with many of the proposed concepts having more than one hull. Speed and payload requirements dictate a lightweight structural design. Optimum structural design depends on an accurate prediction of seaway loads. However, limited sea trial or model test data are available for multi-hull ships.

This report takes measured loads data from model tests and sea trials on catamarans, trimarans, and surface effect ships (SES), and extrapolates them to maximum expected lifetime global loads. This report uses Froude scaling laws for geometrically different ships for each ship and load type using first principles and empirically derived studies. The report then develops simple seaway load prediction algorithms, expressed as functions of ship displacement and various key ship particulars. These global load algorithms are quickly computed, making them suitable for preliminary or concept design studies. They also help guide the ship designer by indicating which ship characteristics most significantly influence the global seaway loads. For completeness, previously developed algorithms for small waterplane area twin hull ships (SWATH) are included in the appendix.

Definition of Variables

Table 1 defines common variables used throughout this paper. Unless otherwise noted, the units are as given in Table 1.

Seaway Loads Definition

This section defines the loads referenced throughout this report. Figure 1 defines the coordinate system with X in the longitudinal direction, Y in the vertical direction, and Z in the transverse direction.

Global Ship Seaway Loads

Figure 1 shows global seaway loads for a monohull ship. These loads also apply to the individual hulls of a multihull ship, or to the entire structure of the multihull ship. The global ship loads are:

- Vertical shear force (VSF): shear force in the Y direction,
- Vertical bending moment (VBM): bending moment about the Z direction (also referred to as hogging and sagging),
- Transverse shear force (TSF): shear force in the Z direction,

- Transverse bending moment (TBM): moment about the Y direction (also referred to as lateral or athwartship bending), and
- Longitudinal torsion moment (LTM): moment about the X direction.

Table 1. Definition of Variables

Variable	Definition	Units
LBP	Length between perpendiculars	ft
B	Beam of single hull	ft
B_{oa}	Beam over all (for multi-hull)	ft
D	Depth	ft
T	Draft	ft
VA	Vertical cross structure moment arm	ft
∇	Displaced volume	ft^3
Δ	Displacement	LTon
ρ	Mass density of water	$slug/ft^3$
g	Acceleration of gravity	ft/s^2
L	Unit of length	ft
t	Unit of time	s
V	Unit of velocity	knots
F	Unit of force	LTon
M	Unit of moment	ft-LTon
P	Unit of pressure	lb/ft^2
Fr	Froude number	non-dim
θ	Heading angle	degrees
$H_{1/3}$	Significant wave height	meters
WD	Wet deck clearance	ft

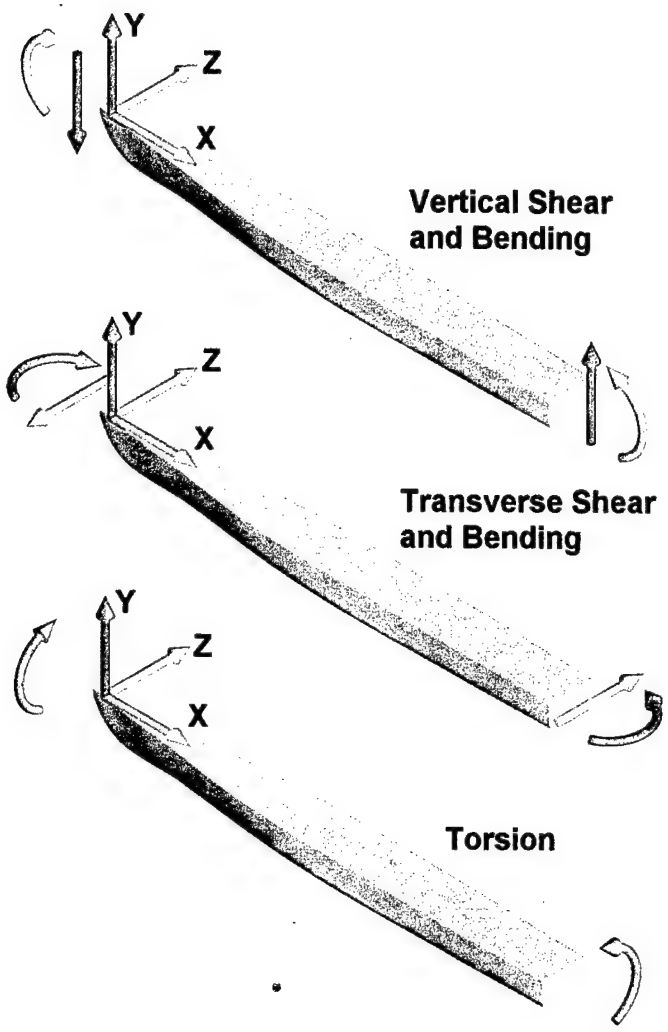

Figure 1. Diagram of Global Ship Loads

Global Cross Structure Seaway Loads

Figure 2 shows global seaway loads which act on a multihull cross structure. These cross structure loads are:

- Heave connection shear force (HCSF): shear force in the Y direction,
- Pitch connection moment (PCM): moment about the Z direction (caused by the relative pitching motion of the hulls),
- Yaw connection moment (YCM): moment about the Y direction (caused by the relative yawing motion of the hulls), and
- Roll connection moment (RCM): moment about the X direction (caused by the relative rolling motion of the hulls).

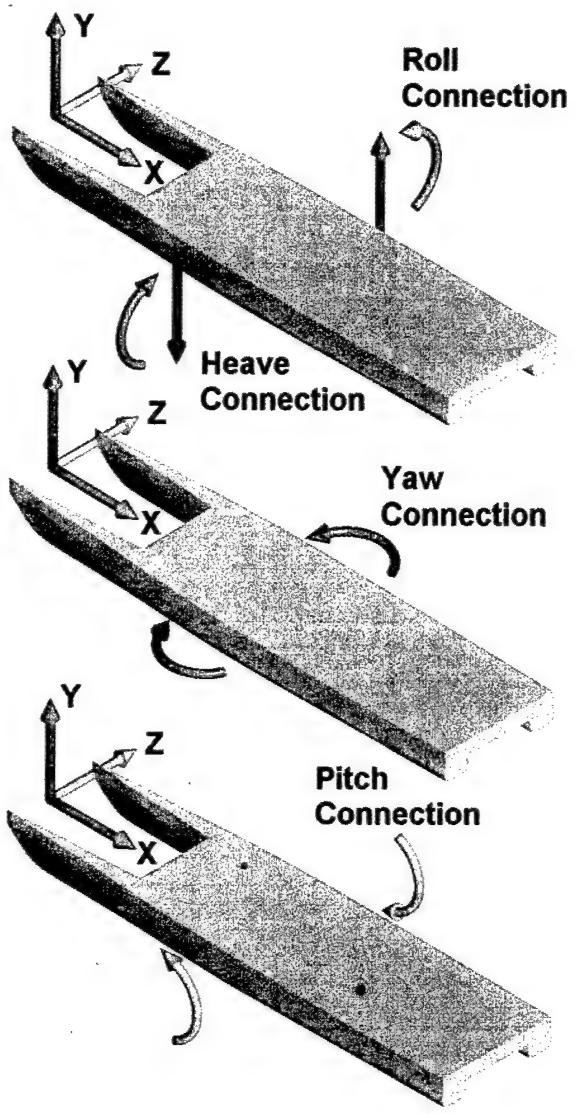

Figure 2. Diagram of Global Cross Structure Loads

This report presents algorithms for predicting vertical bending moments on trimarans and surface effect ships, roll connecting moments on catamarans and trimarans, and pitch connecting moments on catamarans.

Froude Scaling

This report uses Froude scaling to develop algorithms for seaway loads prediction based on model and full-scale test data. Froude scaling is the procedure used for estimating loads of a prototype ship from known loads of an existing ship or model. There are two types of Froude scaling: scaling of a geometrically similar (geosym) model with the same naval architecture coefficients, and scaling of a geometrically dissimilar (non-geosym) model with different naval architecture coefficients. Geosym scaling requires that all dimensions of the model be scaled to

the same linear ratio λ with the prototype. All of the prototype ship characteristics and responses can be determined with this scale factor using the following relationships:

- $L_p/L_m = \lambda$
- $Volume_p/Volume_m = (L_p/L_m)^3 = \lambda^3$
- $Weight_p/Weight_m = (\rho_p g_p/\rho_m g_p)\ (Volume_p/Volume_m) = \lambda^3$ (assumes $\rho_p g_p/\rho_m g_m = 1$)
- $t_p/t_m = (L_p/L_m)^{0.5}\ (g_m/g_p)^{0.5} = \lambda^{0.5}$
- $V_p/V_m = (L_p/L_m)\ /(\ t_p/t_m) = \lambda^{0.5}$
- $F_p/F_m = Weight_p/Weight_m = \lambda^3$
- $M_p/M_m = (F_p/F_m)(L_p/L_m) = \lambda^4$
- $P_p/P_m = (F_p/F_m)/(L_p/L_m)^2 = \lambda$

This report uses data from a literature search of model and full-scale experiment data, as well as data which has not yet been published. Since the data gathered comes from a wide variety of hull forms, this report uses non-geosym scaling. Non-geosym Froude scaling involves determining which hull characteristics influence a particular load, and then scaling the load data based on those characteristics. For vertical bending moments, the length of the ship heavily influences the load, and the non-geosym scaling law is:

$$VBM_p = (LBP_p^3 * B_p)/(LBP_m^3 * B_m) * VBM_m. \quad (1)$$

For the roll connection moment, the submerged profile area, as well as the size of the moment arm, influence the load, and the non-geosym scaling law becomes:

$$RCM_p = (LBP_p * T_p^2 * VA_p)/(LBP_m * T_m^2 * VA_m) * RCM_m. \quad (2)$$

Finally, for the pitch connection moment, the waterplane area and the moment arm created by the length influence the load, and the non-geosym scaling law is:

$$PCM_p = (LBP_p^2 * B_p * \Delta_p^{1/3})/(LBP_m^2 * B_m * \Delta_m^{1/3}) * PCM_m. \quad (3)$$

Catamarans

Although there exist a number of catamarans in service worldwide, there are little data available on measured loads in a seaway. Table 2 summarizes ship particulars for four catamarans with documented seaway load data. All the catamarans listed in Table 2 are models. Table 2 lists their full-scale dimensions for purposes of comparison. This section develops seaway loads algorithms for roll connecting moments and pitch connecting moments from this data.

Table 2. Ship Characteristics of Catamarans Used to Develop Algorithms

Characteristic (units)	ASR	CVA	Stevens Institute	Marintek
Displacement (LTon)	2794	90800	130	3000
LBP (ft)	210	820	99	280
Beam Single Hull (ft)	24	97.3	11.3	20
Beam Overall (ft)	86	237.3	21.3	48.4
Draft (ft)	18	36.5	6	17.4
Vertical Arm (ft)	32.1	79.8	n/a	19.7
Reference	(Lee, Jones, and Curphey 1973)	(Lee, Jones, and Curphey 1973)	(Maniar 1965)	(Hermundstad, Aarsnes, and Moan 1999)

Roll Connection Moments

Catamarans behave similarly to SWATH ships. The roll connection moment, or the prying and spreading of the two hulls, is the most significant primary load. These moments are most severe in beam seas and at zero speed. Before the loads data for the ships in Table 2 can be scaled, the effects of speed and heading must be normalized. Lee et al (1973) conducted parametric studies on the effects of ship speed on roll connection moments for the ASR catamaran model. Figure 3 plots the normalized maximum value of the roll connection moment response amplitude operators (RAO) from ASR as a function of Froude number. Equation 4 presents an algorithm normalizing the roll connection moment based on the Froude number at which the data were measured. The resulting factor, k_{speed}, was used to normalize measured loads at speeds other than zero. Equation 4 assumes that the roll connection moment remains constant above a Froude number of 0.5.

$$k_{speed} = 1.0 - \tanh(1.5*Fr) \quad \text{but not less than } 0.36 \tag{4}$$

Several of the models had test data for different headings. Figure 4 shows normalized loads data from the ASR, Stevens Institute, and Marintek models. Equation 5 presents an algorithm that normalizes the roll connection moment based on the wave heading angle at which the data was measured.

$$k_{heading} = (\sin(\theta))^2 \tag{5}$$

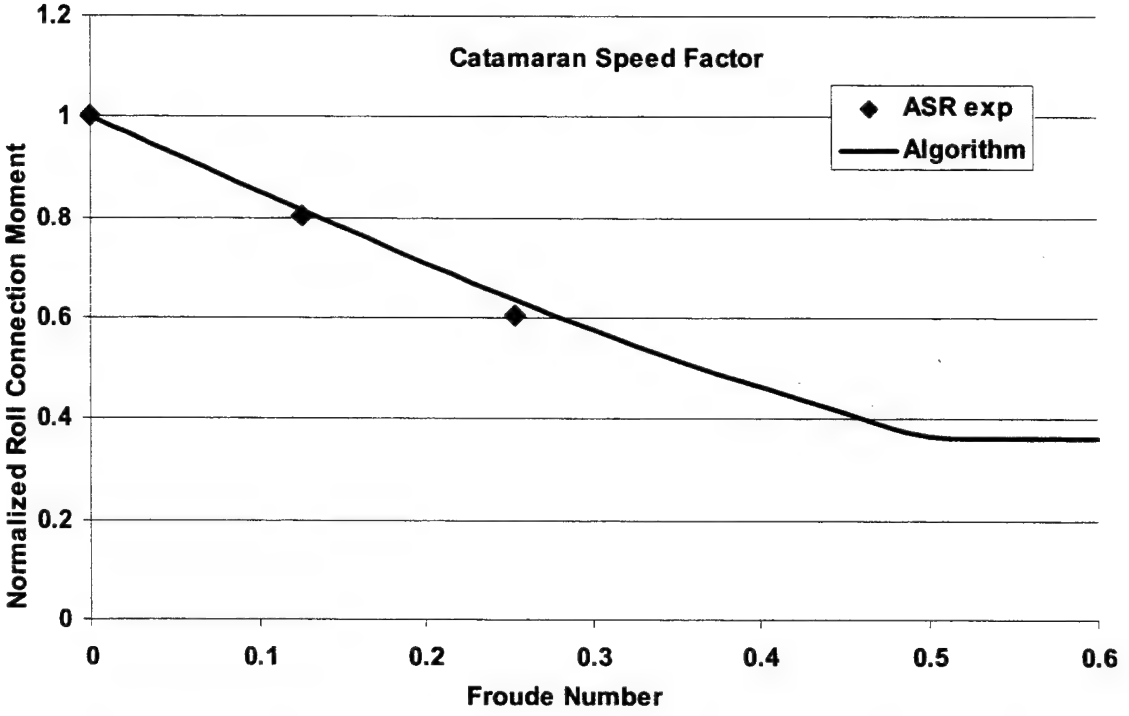

Figure 3. Maximum RCM RAO Value as a Function of Froude Number

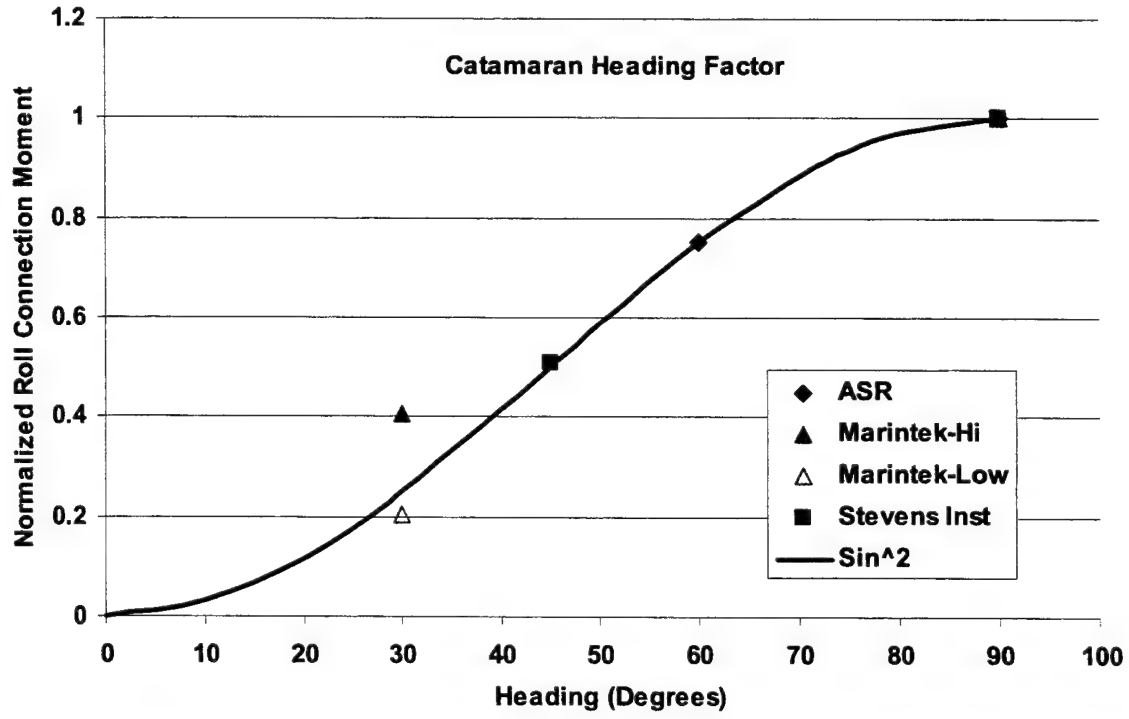

Figure 4. Plot of Maximum RCM RAO Value as a Function of Wave Heading

Figure 5 shows the roll connection moment RAO's for the test data from the models in Table 2. The data in Figure 5 was first non-dimensionalized using the equation,

$$RAO_{RCM}(\text{non-dim}) = RAO_{RCM}/(LBP_m * T_m * VA_m), \quad (6)$$

which was derived from Equation 2, and then normalized for speed and heading using Equations 4 and 5 respectively. Figure 5 shows a generic RAO that reasonably brackets the data.

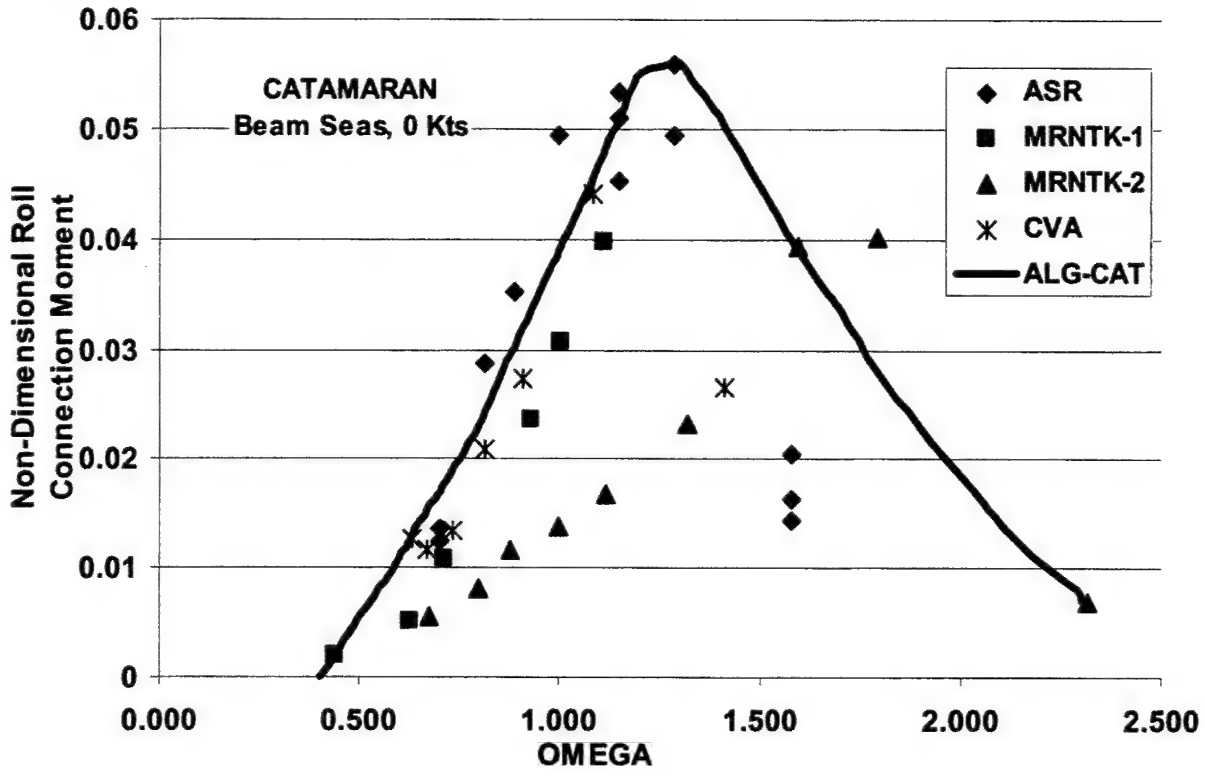

Figure 5. Scaled RAO Data for the Roll Connection Moment

The SPECTRA program (Michaelson 2000) used this generic RAO to predict the most probable lifetime maximum roll connecting moments. A 3600 day at sea lifetime (180 days per year over a 20 year lifetime) was used. Table 3 shows operational profiles for small ships under 10,000 LTons and Table 4 shows operational profiles for large ships greater than 10,000 LTons. Table 5 shows the sea state probabilities used in the analysis. These probabilities correspond to unrestricted operations in the North Atlantic.

Table 3. Operational Profiles SPECTRA Input for Ships < 10,000 LTons

Speed	Heading	$H_{1/3}$ = 0 to 5 m	$H_{1/3}$ = 5 to 10 m	$H_{1/3}$ > 10 m
0	0	0.0311	0.0625	0.4800
0	45	0.0625	0.1250	0.2500
0	90	0.0625	0.1250	0.0100
0	135	0.0625	0.1250	0.2500
0	180	0.0311	0.0625	0.0100
20	0	0.0936	0.0625	0.0
20	45	0.1877	0.1250	0.0
20	90	0.1877	0.1250	0.0
20	135	0.1877	0.1250	0.0
20	180	0.0936	0.0625	0.0

Table 4. Operational Profiles SPECTRA Input for Ships > 10,000 LTons

Speed	Heading	$H_{1/3}$ = 0 to 5 m	$H_{1/3}$ = 5 to 10 m	$H_{1/3}$ > 10 m
0	0	0.0050	0.0625	0.3500
0	45	0.0300	0.1250	0.1250
0	90	0.0300	0.1250	0.1000
0	135	0.0300	0.1250	0.1250
0	180	0.0050	0.0625	0.1000
20	0	0.1000	0.0625	0.1500
20	45	0.2333	0.1250	0.0300
20	90	0.2334	0.1250	0.0
20	135	0.2333	0.1250	0.0200
20	180	0.1000	0.0625	0.0

Table 5. Sea State Probabilities SPECTRA Input

$H_{1/3}$ (m)	North Atlantic	Littoral
0 - 1	0.0503	0.37151
1 - 2	0.2665	0.33521
2 - 3	0.2603	0.16917
3 - 4	0.1757	0.07467
4 - 5	0.1014	0.02792
5 - 6	0.0589	0.01192
6 - 7	0.0346	0.00570
7 - 8	0.0209	0.00204
8 - 9	0.0120	0.00092
9 - 10	0.0079	0.00050
10 - 11	0.0054	0.00024
11 - 12	0.0029	0.00020
12 - 13	0.0016	0.0
13 - 14	0.00074	0.0
14 - 15	0.00045	0.0
> 15	0.00041	0.0

The SPECTRA program multiplies the RAO's for each combination of speed and heading by the sea spectra for each wave height. The program then combines the corresponding Rayleigh probability distributions for each heading, speed, and wave height to form the most probable extreme wave induced load. Figure 6 plots the maximum lifetime roll connection moments for four ship sizes on a logarithmic scale.

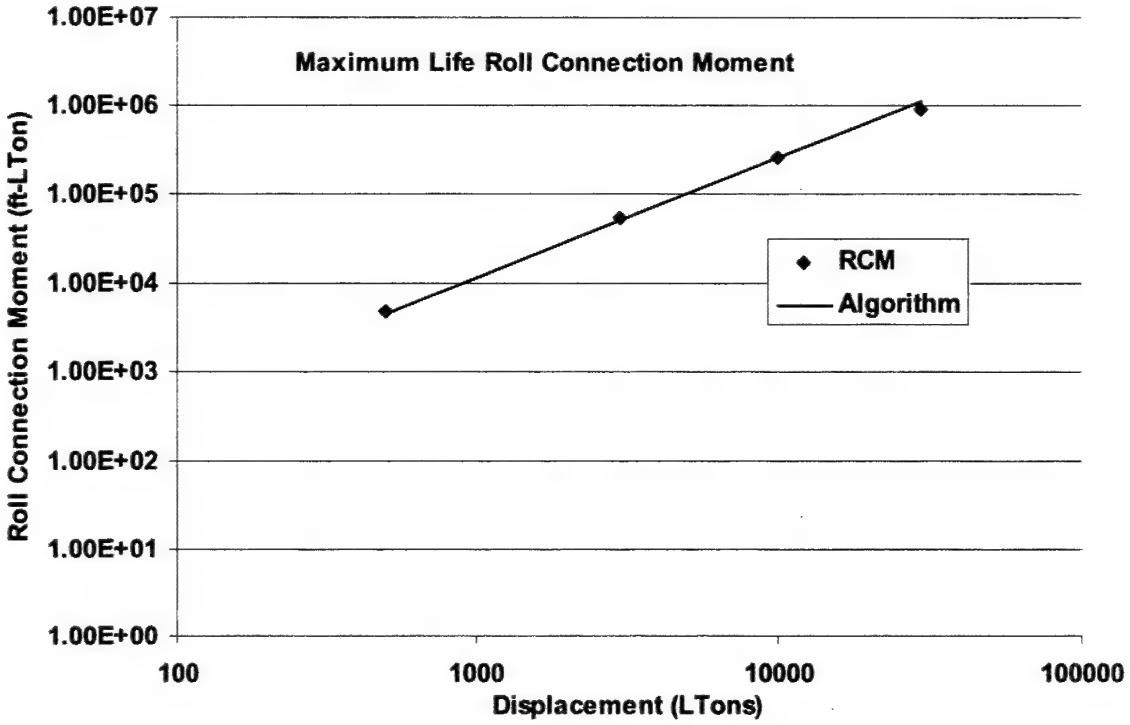

Figure 6. Maximum Predicted Lifetime Roll Connection Moments

Figure 6 also shows a best-fit approximation to the data using the equation,

$$RCM_m = \Delta^{1.35} \tag{7}$$

This equation must now be scaled using the scaling law in Equation 2 to come up with the desired roll connection moment for the prototype ship. Plugging Equation 7 into Equation 2, we get:

$$RCM_p = (LBP_p * T_p^2 * VA_p)/(LBP_m * T_m^2 * VA_m) * \Delta^{1.35} \tag{8}$$

We will use the ASR catamaran as our baseline model. Since the displacement of our prototype ship is not known, we must normalize the ASR dimensions by the cube root of the original displacement. Equation 8 then becomes:

$$RCM_p = (LBP_p * T_p^2 * VA_p)/(14.91 * 1.278^2 * 2.279 * \Delta^{4/3}) * \Delta^{1.35}$$

By making the approximation that $\Delta^{1.35}/\Delta^{1.33} = 1$, the equation becomes:

$$RCM_p = 0.021*LBP_p*T_p^2*VA_p \quad (9)$$

The transverse shear force acting along the length of the hull can be calculated by dividing out the moment arm VA:

$$TSF_p = 0.021*LBP_p*T_p^2 \quad (10)$$

Pitch Connection Moments

The relative pitching motion of the two hulls of a catamaran induces a torsional moment in the cross structure known as the pitch connection moment. The ASR, CVA, Marintek, and Tornton had pitch connection loads experimentally measured and documented in their respective reports. This section uses these measurements to develop an algorithm for predicting the maximum lifetime pitch connection moment on a catamaran of a given size. The reports for the ASR and CVA models documented pitch connection moments response amplitude operators (RAO) at various headings and speeds. Figure 7 and Figure 8 compare the maximum measured RAO for the ASR and CVA models at various speeds and headings.

Figure 7 shows that the pitch connection moment does not vary appreciably with speed. Figure 8 shows that the pitch connection moment does vary with heading, with a maximum moment occurring in quartering seas. Equation 11 below calculates a factor for the pitch connection moment based on the heading. This equation is plotted in Figure 8.

$$F_{heading}(\theta) = 0.75 - 0.3*\cos(\pi/90*\theta) - 0.25*\cos(\pi/45*\theta), \text{ not greater than 1} \quad (11)$$

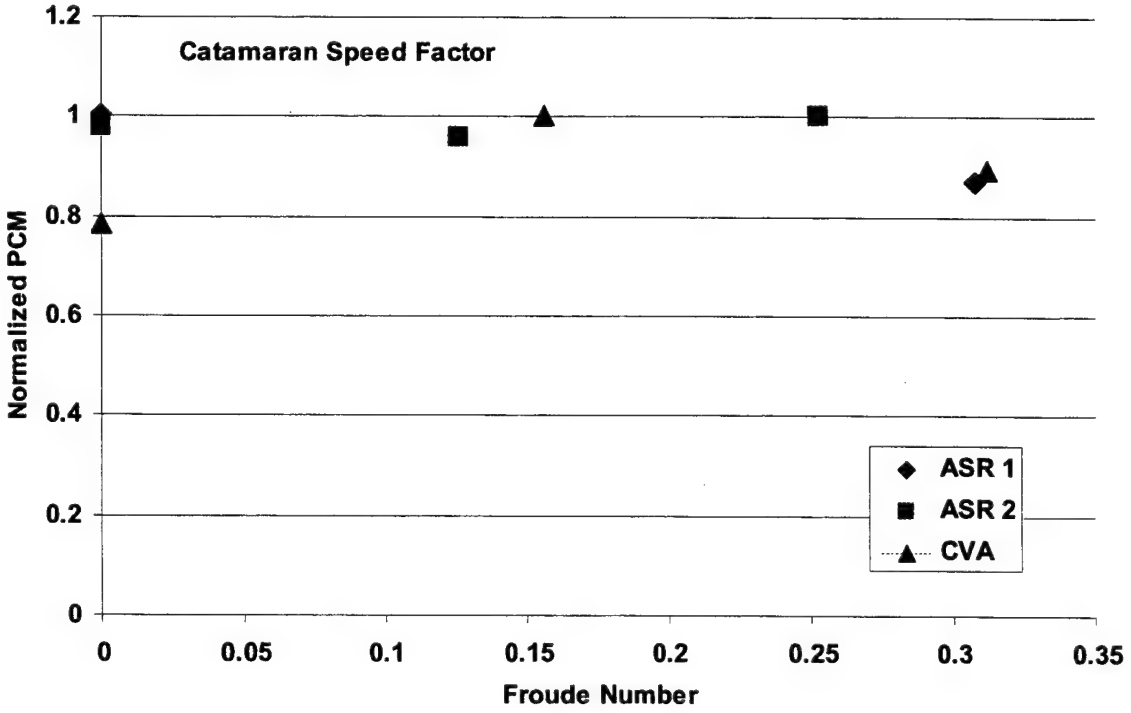

Figure 7. Maximum PCM RAO Value as a Function of Froude Number

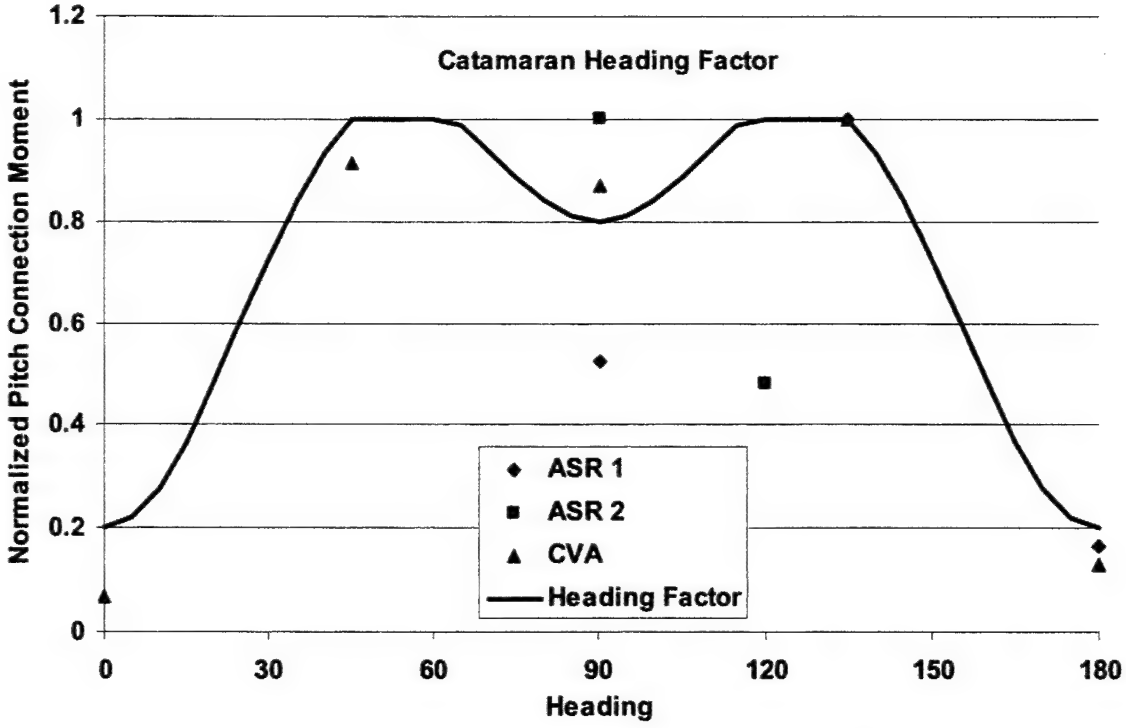

Figure 8. Maximum PCM RAO Value as a Function of Wave Heading

Figure 9 shows the pitch connection moment RAO's for the test data from some of the models in Table 2. The data in Figure 9 was first non-dimensionalized using the equation

$$RAO_{PCM}(\text{non-dim}) = RAO_{PCM}/(LBP_m^2 * B_m) \tag{12}$$

which was derived from Equation 3, and then normalized for heading angle using Equation 11. Figure 9 shows a generic RAO that reasonably brackets the data.

The SPECTRA program (Michaelson 2000) used this generic RAO to predict the most probable lifetime maximum pitch connection moment. The same SPECTRA inputs as previously used for the roll connection moment were used for the pitch connection moment predictions. Figure 10 plots the maximum lifetime pitch connection moments for four ship sizes.

Figure 10 also shows a best-fit approximation to the data using the equation,

$$PCM_m = 8.27 * \Delta \tag{13}$$

This equation must now be scaled using the scaling law in Equation 3 to come up with the desired pitch connection moment for the prototype ship. Plugging Equation 13 into Equation 3, we get:

$$PCM_p = (LBP_p^2 * B_p * \Delta_p^{1/3})/(LBP_m^2 * B_m * \Delta_m^{1/3}) * 8.27 * \Delta \tag{14}$$

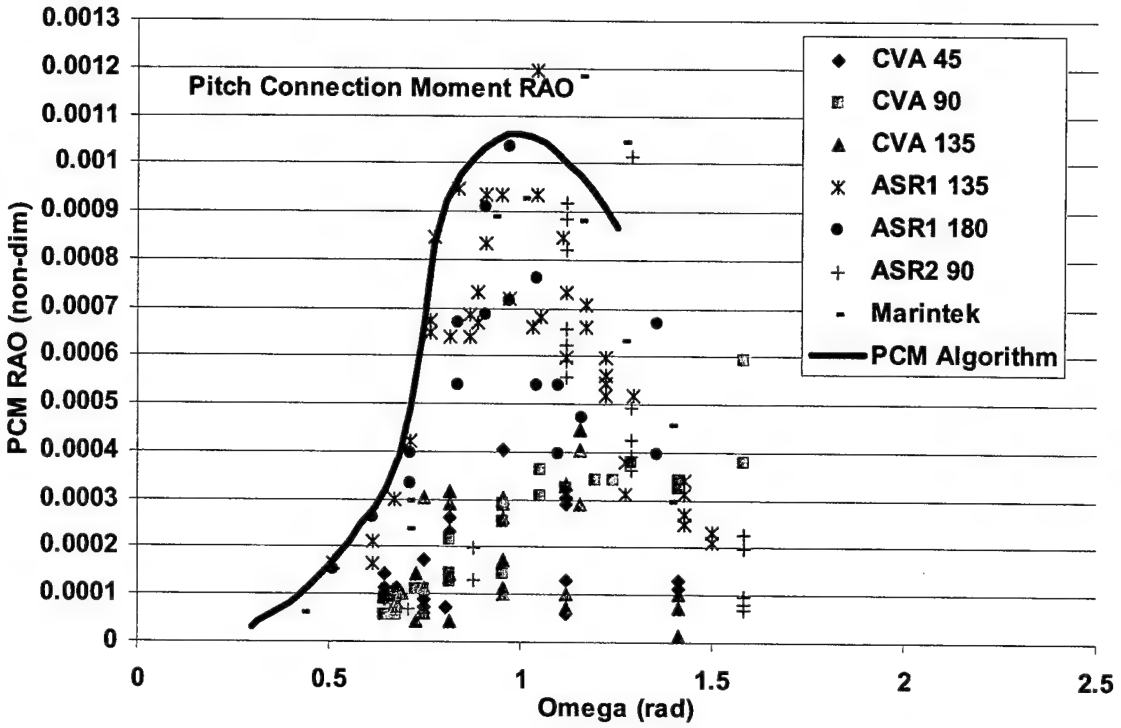

Figure 9. Scaled RAO Data for the Pitch Connection Moment

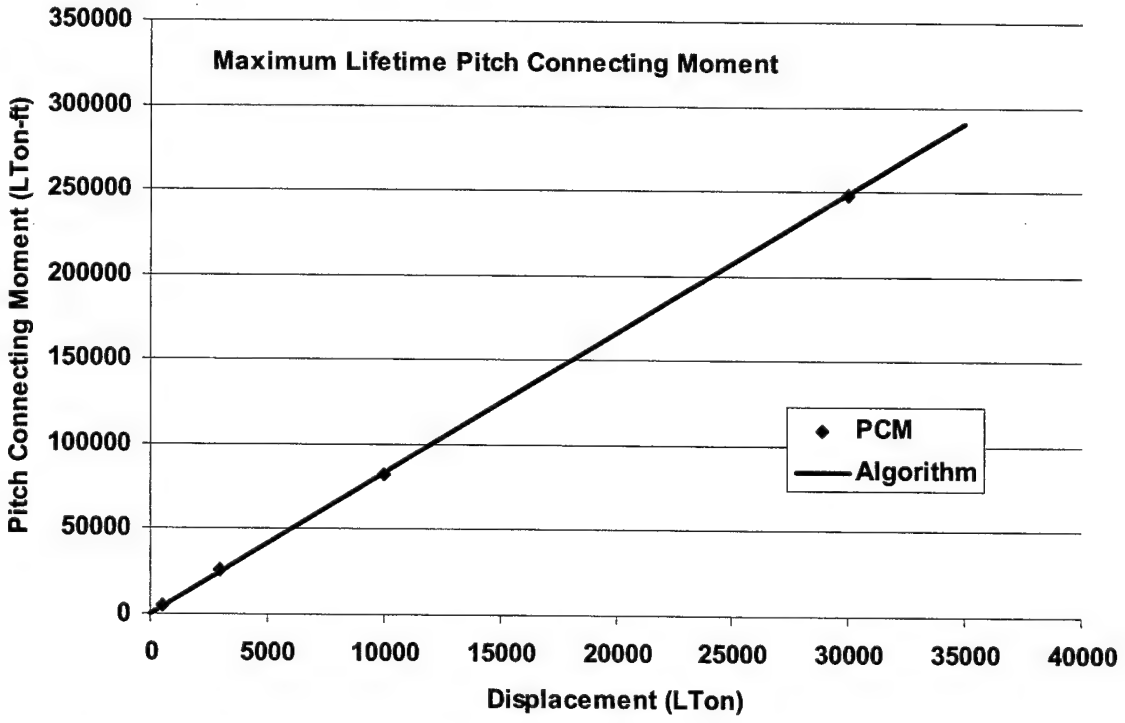

Figure 10. Maximum Predicted Lifetime Pitch Connection Moments

We will use the ASR catamaran as our baseline model. Since the displacement of our prototype ship is not known, we must normalize the ASR dimensions by the cube root of the original displacement. Equation 14 then becomes:

$$PCM_p = (LBP_p^2 * B_p * \Delta_p^{1/3}) / (14.91^2 * 1.704 * 1 * \Delta^{4/3}) * 8.27 * \Delta$$

By evaluating the above equation and canceling terms, we come up with our final algorithm:

$$PCM_p = 0.0217 * LBP_p^2 * B_p \quad (15)$$

Littoral Operations Reduction

The algorithms developed above are for unrestricted operations in the open ocean. Frequently, smaller catamarans are designed to only operate in the littoral. Table 5 presents sea state probabilities for a nominal littoral scenario, with one fifth of the time assumed in each of these areas: East Coast of the U.S., eastern Mediteranean Sea, Persian Gulf, Northwest Indian Ocean, and the Gulf of Mexico northwest of Haiti. The ship designer may desire to further restrict operations to sea state 5 (4 meters maximum), sea state 6 (6 meters maximum), or sea state 7 (9 meters maximum). Figure 11 shows the maximum lifetime roll connecting moments for the 500-LTon variant of the ASR catamaran in littoral operations at various significant wave height restrictions. The following load reduction factor fits the data shown in Figure 11 and can be used as a multiplication factor to account for load reduction in the littoral,

$$k_{littoral} = 0.88 - 0.0059(H_{1/3} - 12)^2 \quad (16)$$

where $H_{1/3}$ is the significant wave height in meters. A maximum 12-meter wave height occurs in the littoral.

Trimarans

There exist few trimaran models and ships for which there are measured loads data. Table 6 presents the ship particulars for three different trimaran configurations. The RV Triton is a 1267-LTon trimaran with a frigate bow and v-shaped side hulls (Figure 12). The side hulls extend 38% of the center hull length and are centered around midships. Sea trials were conducted in the North Atlantic during 2002.[1] The O'Neil hull form (OHF) model (Kihl 1989; Lamb 2003) represented a 3400 LTon combatant with small waterplane area hulls (Figure 13). The center hull extends slightly forward of the leading edges of the side hulls, and the side hulls extend aft of the center hull transom. The High-Speed Sealift (HSS) model is a 21,000 LTon trans-oceanic transporter (Rodd, 2003)[2] having a long, slender center hull (L/B = 16.6) with a

[1] Grassman, J. Matthew, *Structural Sea Trials and Finite Element Modeling of RV* Triton *Trimaran* , a report in preparation by NSWCCD.

[2] Rodd, James, *Seaway Induced Loads Obtained from a Segmented Model of High-Speed Sealift Trimaran Model 5594*", a report in preparation by NSWCCD.

wave-piercing bow (Figure 14). The side hulls are only 14% of the center hull length and are located at the extreme aft end of the ship.

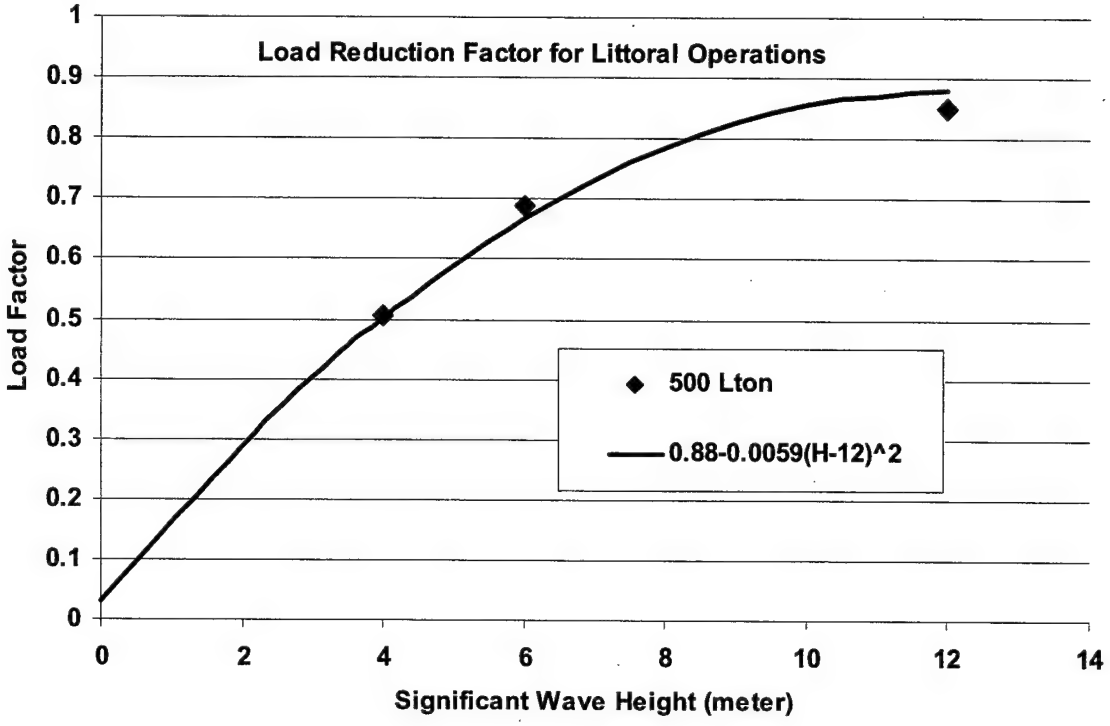

Figure 11. Effects of Operating Restrictions on Catamaran Loads

Table 6. Ship Characteristics of Trimarans Used to Develop Algorithms

Displacement (units)	RV *Triton*	O'Neil Hull Form	High-Speed Sealift
Total (LTon)	1267	3429	21653
Center Hull			
Length (ft)	295.3	222	1026.9
Beam (ft)	23	6.5	61.7
Draft (ft)	11.48	25.1	30.8
Side Hulls			
Disp. (both hulls) (LTon)	115	1456	880
Length (ft)	111.5	261.5 (hull), 180 (strut)	147.6
Beam (ft)	4.6	11	9.8
Draft (ft)	7.87	18.5	21.3
Reference	See footnote 1, page 14.	(Lamb 2003)	See footnote 2, page 14.

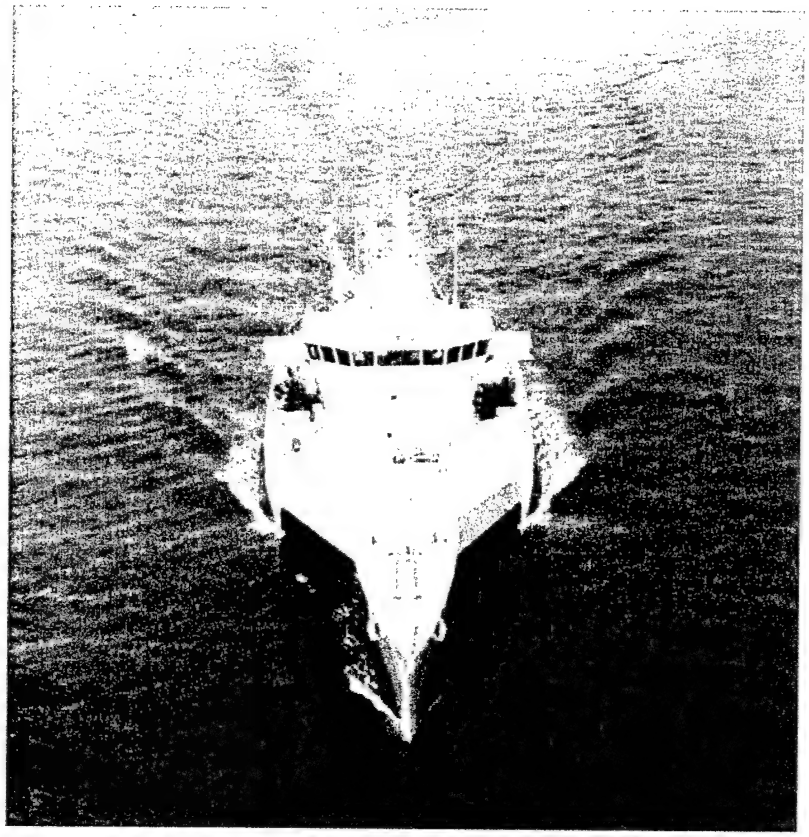

Figure 12. RV Triton

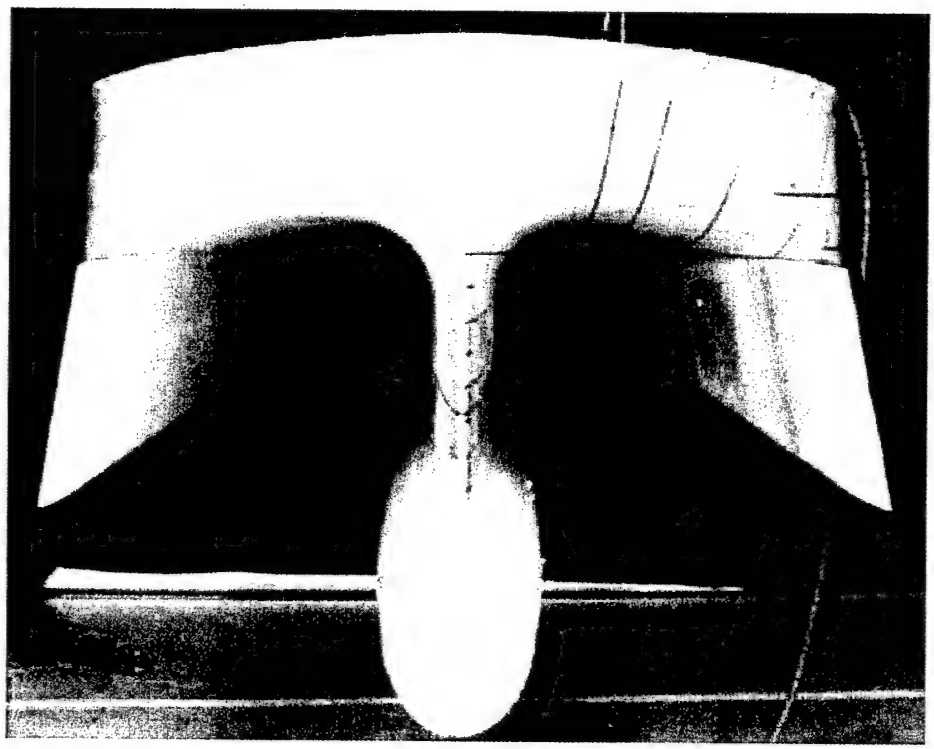

Figure 13. O'Neil Hull Form Model

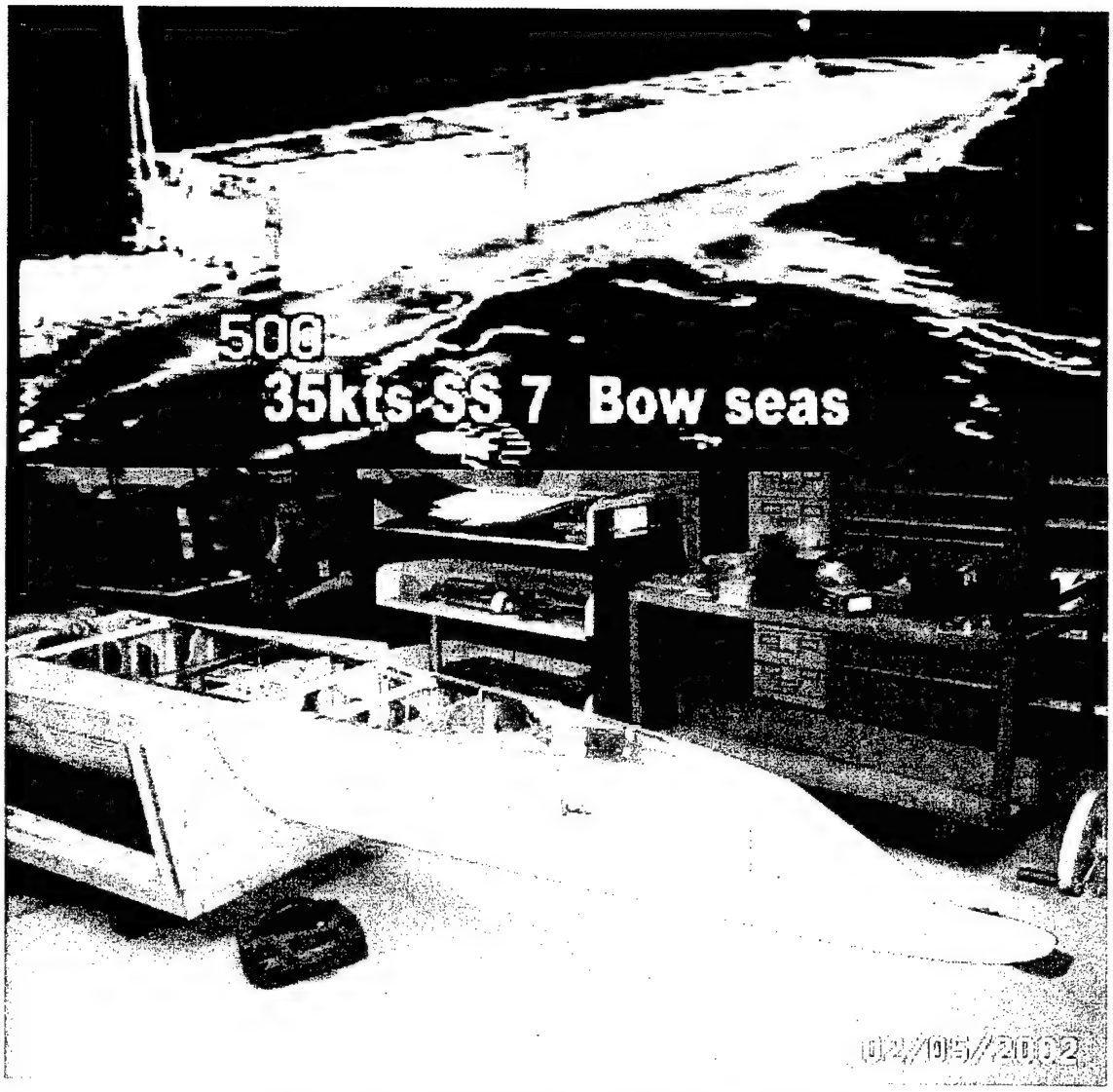

Figure 14. High-Speed Sealift (HSS) Model

Side Forces on Side Hulls

The roll connection moment, or the prying and spreading of the two hulls, can be the most significant primary loading on trimarans, depending upon their relative length to the center hull. These moments result from side forces acting at the mid-draft of the side hulls, and are most severe in beam seas.

In order to generate design loads, the measured roll connecting moments and side forces from different sized ships and models must be compared on a common basis. The moment and force response amplitude operators for each of the three ships were Froude scaled to ship sizes of 500 LTons, 3000 LTons, 10000 LTons, and 30000 LTons using the following equation derived from Equation 2 above:

$$RAO_p = (LBP_p * T_p)/(LBP_m * T_m) * RAO_m. \quad (17)$$

These scaled RAO's were input into the seaway loads prediction program SPECTRA to determine the maximum expected lifetime loads. The other SPECTRA inputs were the same as those used for the catamaran loads prediction algorithms above. Figure 15 plots the maximum expected lifetime side forces as a function of the side hull displacement on a logarithmic scale. Figure 15 shows that the O'Neil hull form follows a distinct trend from the Triton and the HSS, most likely due to its unique hull form. Because of this difference, two separate load algorithms are required – one for a typical trimaran hull form and another for the O'Neil hull form.

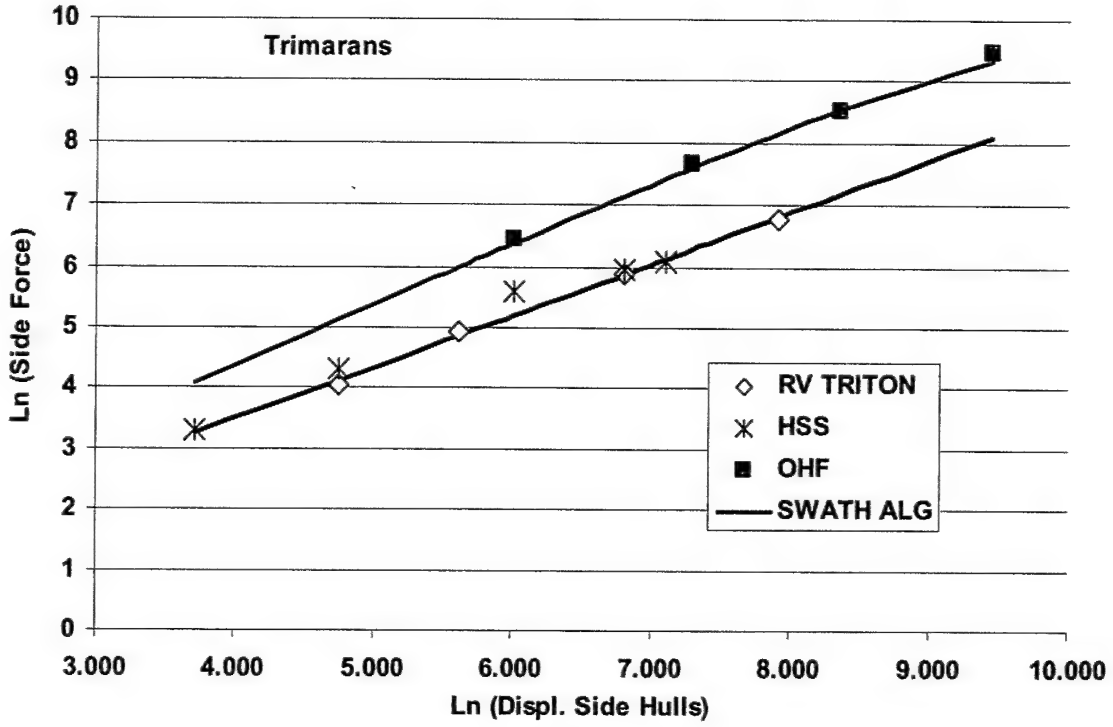

Figure 15. Maximum Expected Lifetime Side Force on Side Hulls

Typical Trimaran

Figure 15 shows a best-fit approximation for the typical hull form data using the equation

$$TSF_{trimaran} = 1.127 * (\Delta_{side\ hull})^{0.844} \quad (18)$$

This equation must now be scaled by adapting the scaling law in Equation 2 to come up with the side force for the prototype ship. Plugging Equation 18 into Equation 2, and removing the vertical moment arm term, we get:

$$TSF_p = (LBP_p * T_p^2)/(LBP_m * T_m^2) * 1.127 * \Delta^{0.844} \quad (19)$$

We will use the RV *Triton* trimaran as our baseline model. Since the displacement of our prototype ship is not known, we must normalize the *Triton* side hull dimensions by the cube root of the original displacement of the side hulls. Equation 19 then becomes:

$$TSF_p = (LBP_p * T_p^2)/(22.93 * 1.62^2 * \Delta) * 1.127 * \Delta^{0.844}$$

By evaluating the above expression, the equation becomes:

$$TSF_p = 0.0187 * LBP_p * T_p^2 / \Delta^{0.156} \quad (20)$$

O'Neil Hull Form

The side hulls of the O'Neil hull form are SWATH-like and provide a much larger portion of the total ship displacement than other trimarans. Because of this, Equation 18 underpredicts the expected side forces on the OHF. However, a simplified version of the SWATH side load algorithm derived in Appendix A fits the data in Figure 15 well,

$$SF_{OHF} = (\Delta_{side\ hull}) * k_d * k_l * k_t \quad (21)$$

where,

$$k_d = 1.55 - 0.75 * \tanh(\Delta_{side\ hull}/11{,}000)$$

$$k_l = 0.75 + 0.35 * \tanh(0.5 * LBP_{side\ hull}/(\Delta_{side\ hull})^{1/3} - 6)$$

$$k_t = 0.5319 * T_{side\ hull}/(\Delta_{side\ hull})^{1/3}$$

Vertical Bending Moment of Center Hull

Figure 16 shows the RAO data for the vertical bending moment on the RV Triton, and Figure 17 shows the RAO data for the High Speed Sealift model.

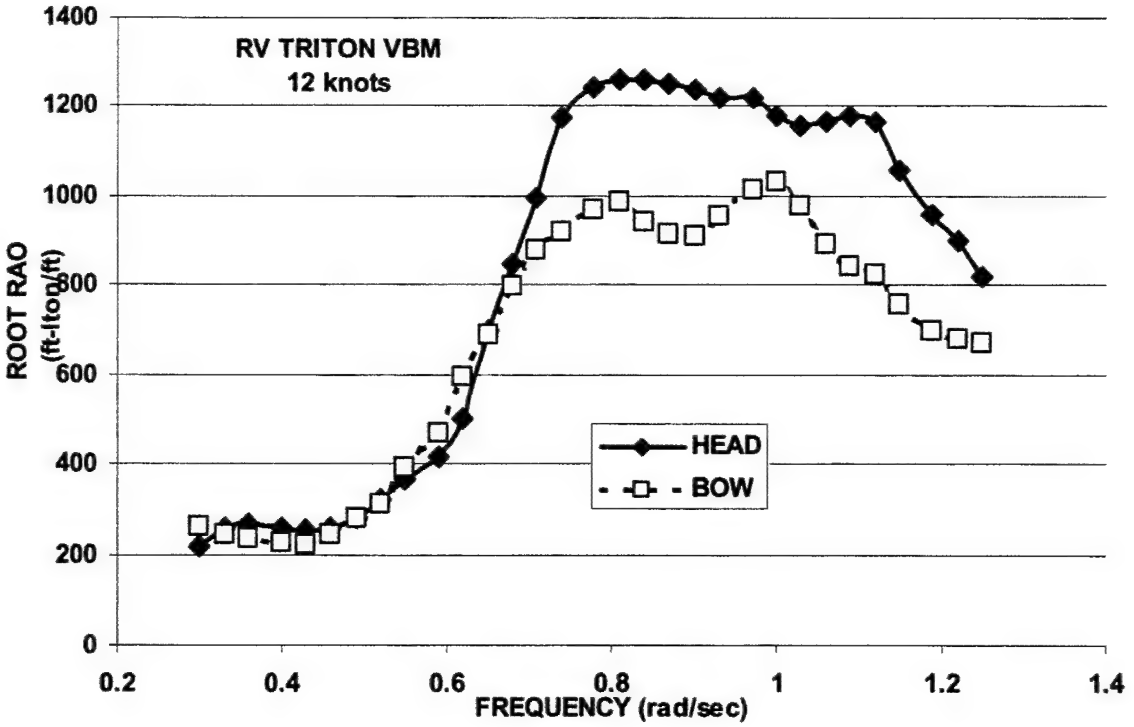

Figure 16. RAO Data for RV Triton Vertical Bending Moment

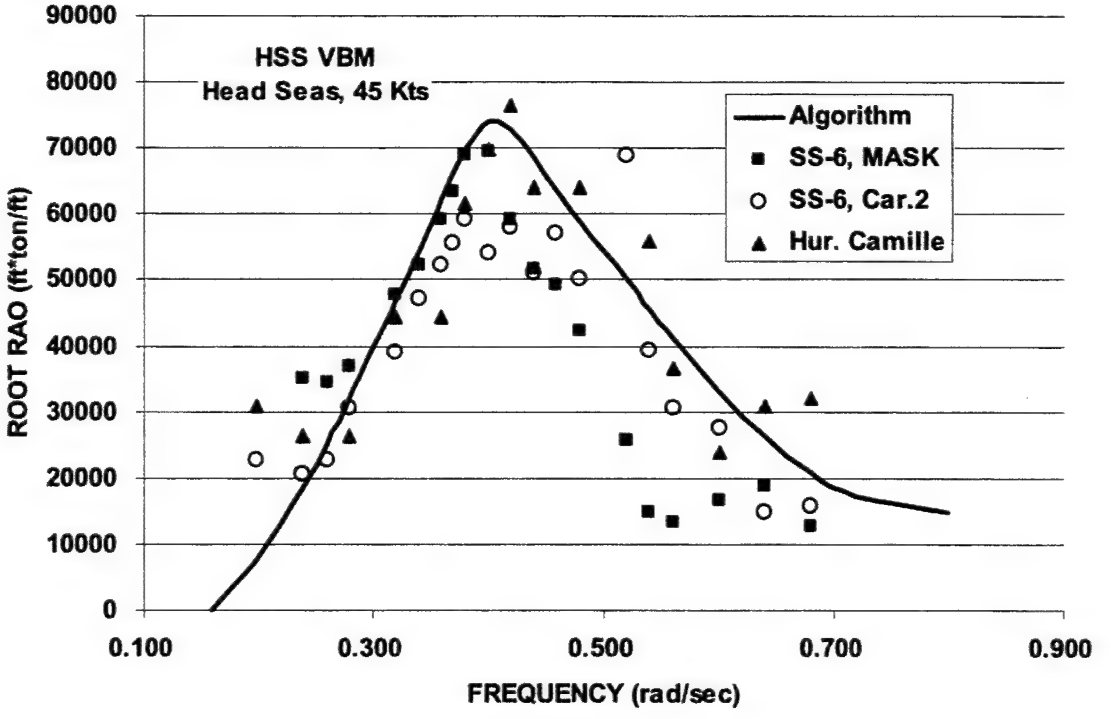

Figure 17. RAO Data for High-Speed Sealift (HSS) Vertical Bending Moment

These RAO's were input into the seaway loads prediction program SPECTRA to determine the maximum expected lifetime loads. The other SPECTRA inputs were the same as those used for the catamaran loads prediction algorithms above. Since the *Triton* center hull has a traditional frigate V-shaped bow and the HSS hull form has a wave piercing bow that reduces vertical bending moments, two distinct loading algorithms are required to predict the maximum expected lifetime vertical bending moment for the hulls.

Frigate Shaped Bow Hull Form

Using Equation 1 above, and substituting the RV *Triton* parameters for LBP_m, B_m, and VBM_m as predicted by SPECTRA, we can derive the vertical bending moment algorithm for a trimaran with conventional V-shaped bow as:

$$VBM_p = (LBP_p^3 * B_p)/(295.3^3 * 23) * 30{,}650$$

$$VBM_p = 0.0000517 * LBP_p^3 * B_p \tag{22}$$

Wave Piercing Bow Hull Form

Using Equation 1 above, and substituting the HSS parameters for LBP_m, B_m, and VBM_m as predicted by SPECTRA, we can derive the vertical bending moment algorithm for a trimaran with wave piercing bow as:

$$VBM_p = (LBP_p^3 * B_p)/(1026.9^3 * 61.7) * 1{,}803{,}300$$

$$VBM_p = 0.0000356 * LBP_p^3 * B_p \tag{23}$$

Longitudinal Distribution of Loads

The vertical bending moment algorithms derived above provide the moment amplitude at midships. From the model tests on the HSS (See footnote 2, page 14), the following load reduction factor is appropriate at other longitudinal locations (Figure 18):

$$k_l = 1 - \cos(\pi * x/LBP) \tag{24}$$

where x is the longitudinal location desired.

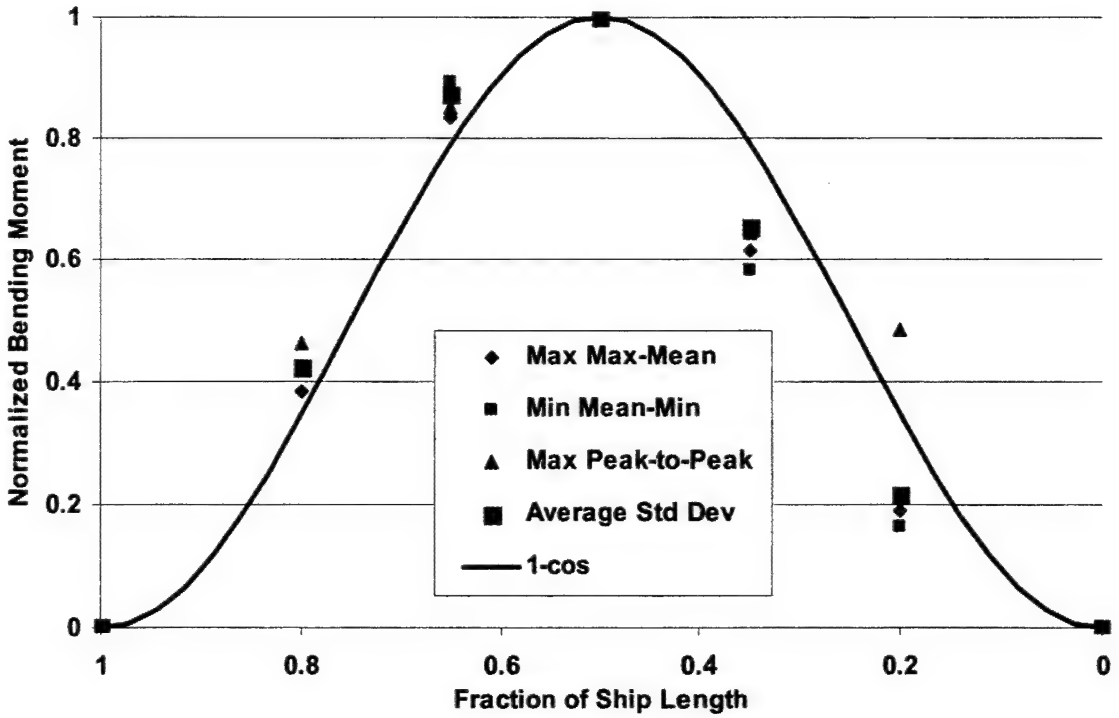

Figure 18. Longitudinal Distribution of Trimaran Vertical Bending Moment

Surface Effect Ships

Although the surface effect ship (SES) concept has been around for decades, there are little data on measured loads in a seaway. Table 7 summarizes ship particulars for three model tested at the David Taylor Model Basin during the 1970s and 1980s. These models were tested in different configurations as part of a parametric test program. For comparison purposes, they are all scaled to a nominal 3000-LTon displacement. Table 7 also shows ship characteristics for the SES-200 catamaran.

Table 7. Ship Characteristics for SESs Used to Develop Algorithms

Characteristic	L/B 7.7	L/B 5	German FTC	SES-200
Displacement (LTon)	3000	3000	3000	205
Length				
Sidehull (ft)	392.5	337	318	141.7
Cushion (ft)	361.5	318	283	131.8
Beam				
Cushion (ft)	47	63.5	60	31
Side Hull (ft)	19	-	-	4
Overall (ft)	85	-	-	39
Draft (off cushion) (ft)	14.4	13.75, 25.0	15.9	-
Wet deck clearance (ft)	4.6	3.0	6.7	1.2
Bow ramp angle (deg)	22	25	12	13.8

Vertical Bending Moment

The vertical bending moment governs the design of the SES global structure. Extensive sea trials and model tests found that the most severe moments occurred off cushion in high seas. Bifurcated Weibull probability distributions were fit to the combined wave and slam induced bending moments from low speed, off cushion test data on the L/B 7.7 model. These Weibull distributions were Froude scaled to 500-, 3000-, 10000- and 30000-LTon ships. Maximum expected lifetime bending moments were calculated for a 20-year lifetime operating in the North Atlantic. It was assumed that the ship was hull borne 20 percent of the time. Figure 19 shows the maximum sagging moments for geosyms of the L/B 7.7.

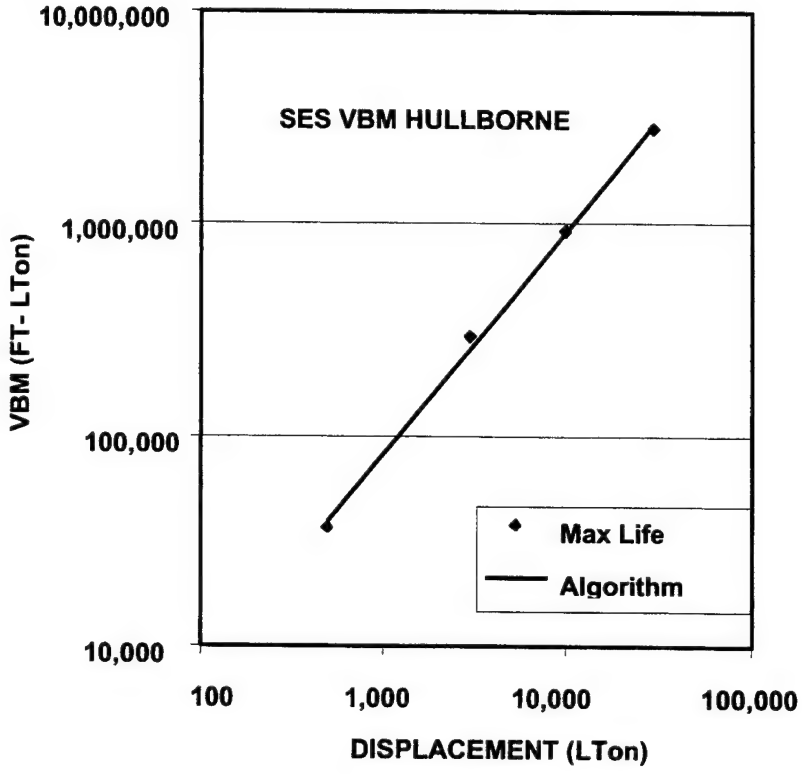

Figure 19. Maximum Sagging Bending Moments for Surface Effect Ships

Figure 19 also shows the following algorithm for predicting the maximum expected lifetime bending moment based on the displacement of the SES:

$$VBM = (40*\Delta)^{1.062} \tag{25}$$

This equation must now be scaled by adapting the scaling law in Equation 1 to come up with the vertical bending moment for the prototype ship. Plugging Equation 25 into Equation 1, we get:

$$VBM_p = (LBP_p^{\,3}*B_p)/(LBP_m^{\,3}*B_m)* (40*\Delta)^{1.062} \tag{26}$$

Here we define LBP as the length of the side hull, and B as the beam of the cushion. We will use the L/B 7.7 SES as our baseline model. Since the displacement of our prototype ship is not

known, we must normalize the SES hull dimensions by the cube root of the original displacement of the ship. Equation 26 then becomes:

$$VBM_p = (LBP_p^3 * B_p)/(27.107^3 * 3.249 * \Delta^{4/3}) * (40*\Delta)^{1.062}$$

By evaluating the above expression, the equation becomes:

$$VBM_p = (0.000777 * LBP_p^3 * B_p)/\Delta^{0.2713} \quad (27)$$

Longitudinal Distribution of Loads

Figure 20 shows data for the longitudinal distribution factor of the vertical bending moment for a SES hull off cushion with a varying amount of wet deck clearance. Figure 20 also shows the following algorithm that fits the data and calculates a multiplication factor for the vertical bending moment to account for the longitudinal location of the load.

$$k_{long} = 2.5*x/LBP \text{ for } x/LBP < 0.4 \quad (28)$$

$$k_{long} = 1.0 \text{ for } 0.4 < x/LBP < 0.5$$

$$k_{long} = 2.0 - 2*x/LBP \text{ for } x/LBP > 0.5$$

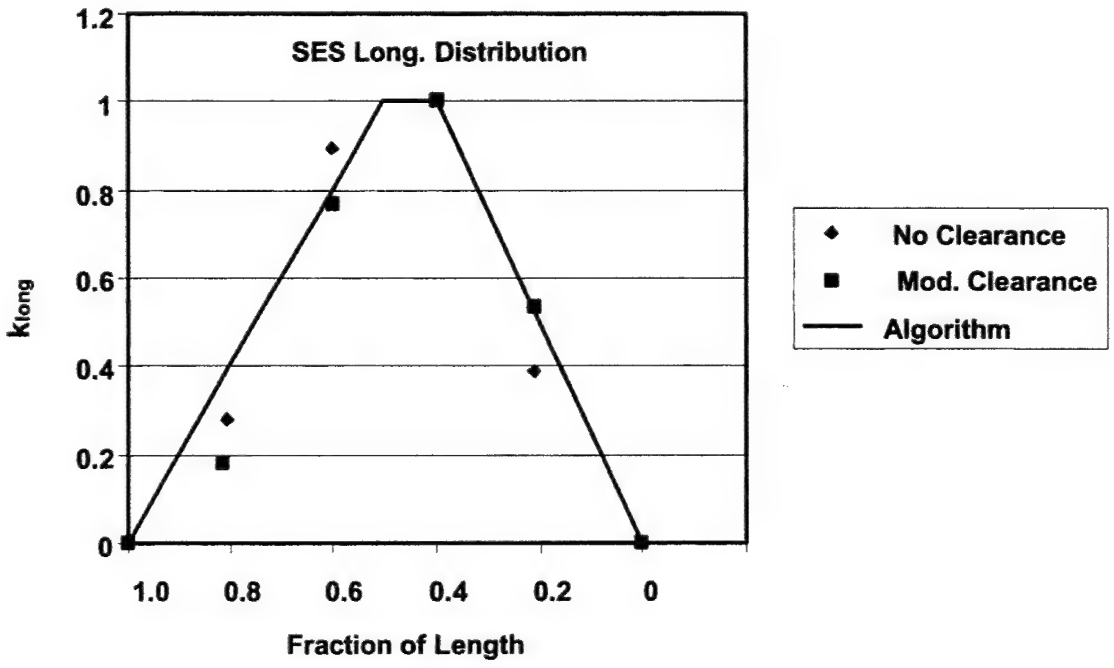

Figure 20. Longitudinal Distribution of Moment on Surface Effect Ships

Effect of Bow Ramp Angle

A portion of the vertical bending moment comes from the impact of the bow and wet deck upon the waves. Richardson (1981) showed that the amplitude of the slam-induced bending moment is related to the impact angle. Figure 21 shows the following algorithm for predicting a load magnification factor based on the ramp angle of the bow:

$$k_{br} = 0.404/\tan(\alpha) \tag{29}$$

where α is the bow ramp angle, and k_{br} is the load magnification factor. The algorithm is valid for bow angles ranging from 10 to 25 degrees. Care should be taken when extrapolating the algorithm outside of this range.

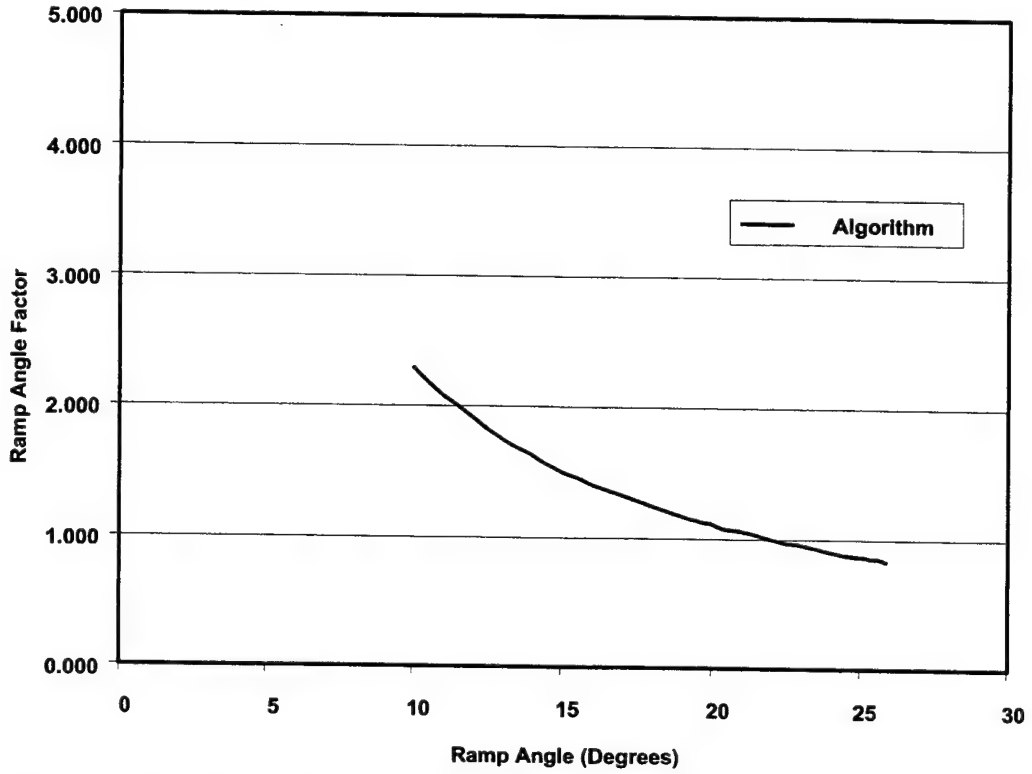

Figure 21. Longitudinal Bending Moment Factor for Bow Ramp Angle on SES

Effect of Freeboard

The clearance between the water's surface and the wet deck, or freeboard, also influences the magnitude of the slamming vertical bending moment. The vertical bending moment for the L/B 7.7 model was measured at different values of freeboard. Figure 22 shows the following algorithm based on the measurements from the L/B 7.7 model tests:

$$k_{wd} = 1.0 + 0.85*(WD/\Delta^{1/3} - 1.0)^2 \tag{30}$$

This load magnification factor is valid only for values of $WD/\Delta^{1/3}$ up to 1.0.

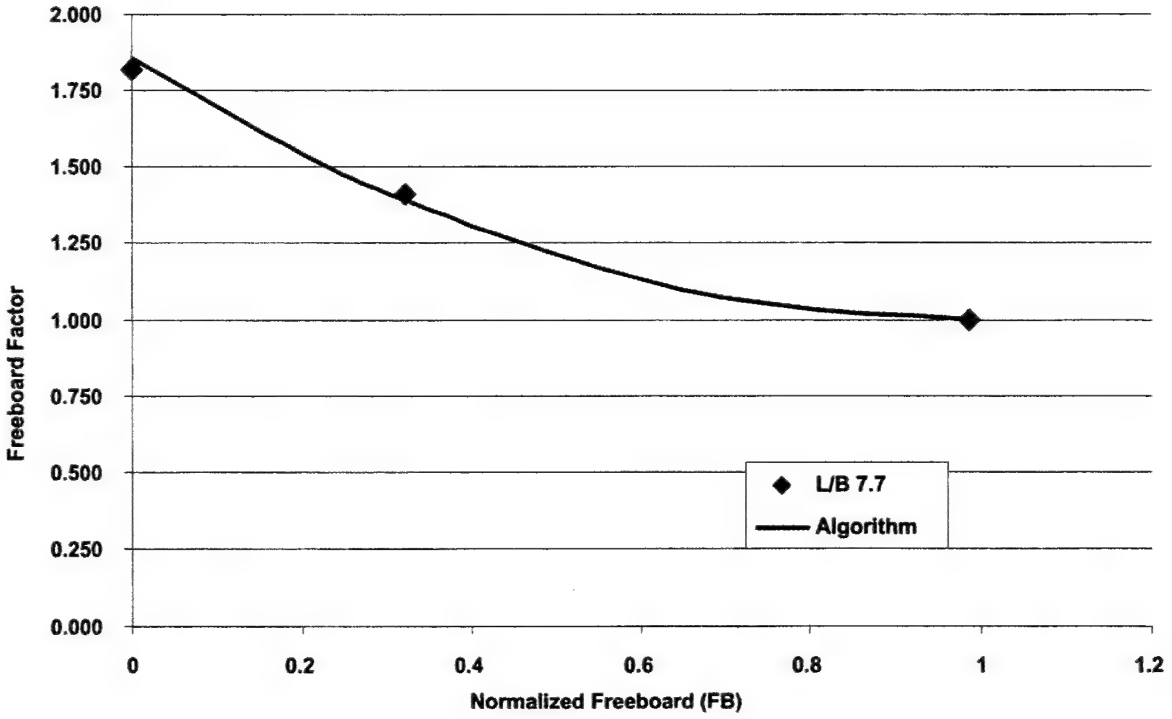

Figure 22. Longitudinal Bending Moment Factor for Freeboard on SES

Effect of Nominal Wave Height

The vertical bending moments are approximately proportional to the significant wave height. Figure 23 plots the following algorithm for predicting the vertical bending moment magnification factor based on the significant wave height:

$$k_{wh} = H_{1/3}/(6.3 + 0.0024*\Delta) \text{ for } \Delta < 3833 \text{ LTons} \quad (31)$$

$$k_{wh} = H_{1/3} \text{ for } \Delta > 3833 \text{ LTons}$$

This algorithm can be used to adjust the predicted vertical bending moments for operations on the littoral or where seas are more severe.

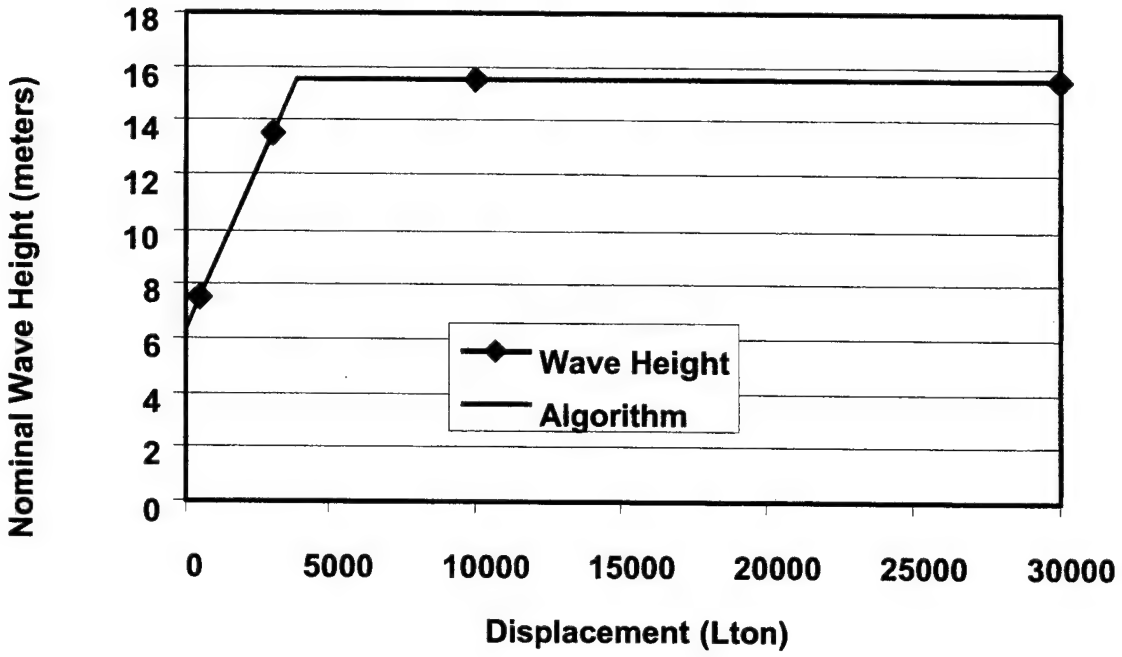

Figure 23. Longitudinal Bending Moment Factor for Nominal Wave Height on SES

Conclusion

This report generated several seaway load prediction algorithms for catamarans, trimarans, and surface effect ships based on available model and full-scale test data. These algorithms are intended for use as quick predictions of seaway loads during ship feasibility and concept design studies. As the ship design progresses and is refined, more accurate but time consuming computational analyses and model tests are appropriate. In some cases algorithms were developed from a minimum amount of data, and it is anticipated that as more data is gathered in the future, these algorithms will be further refined.

References

Hermundstad, O., J. Aarsnes, and T. Moan. 1999. Linear Hydroelastic Analysis of High-Speed Catamarans and Monohulls. *Journal of Ship Research* March 1999.

Kihl, D. 1989. *Primary Structural Load Estimates for an O'Neil Hull Form Ship Based on Model Tests*, SSPD-89-173-26, January 1989. Bethesda, Maryland: David Taylor Research Center.

Lamb, G. R. 2003. Investigation of a Small-Waterplane-Area Trimaran High-Speed Hullform. In *NSWCCD Tehcnical Digest*. West Bethesda, Maryland: Naval Surface Warfare Center, Carderock Division.

Lee, C. M., H. Jones, and R. Curphey. 1973. Prediction of Motion and Hydrodynamic Loads of Catamarans. Paper read at SNAME Chesapeake Section Meeting, March 1973.

Maniar, N. 1965. *Motions and Structural Loading of a 106 Ft. Catamaran in Irregular Waves*, Davidson Laboratory Report 823, January 1965. Hoboken, New Jersey: Stevens Institute of Technology.

Michaelson, R. 2000. *User's Guide for SPECTRA - Version 8.3*, NSWCCD-65-TR-2000/7, West Bethesda, MD: Naval Surface Warfare Center, Carderock Division.

Richardson, W., J. Krouse, and S. Chorney. 1981. *Structural Load Tests on a Length-to-Beam 5 Surface Effect Ship Model*, DTNSRDC report, February 1981. Bethesda, Maryland: David Taylor Naval Ship Research and Development Center.

Sikora, J. 1995. Design Algorithms for Primary and Secondary Loads on SWATH Ships. *Naval Eng. Journal* (May, 1995).

Sikora, J., A. Dinsenbacher, and J. Beach. 1983. A Method for Estimating Lifetime Loads and Fatigue Lives for SWATH and Conventional Monohull Ships. *Naval Engineers Journal* 95 (3).

Appendix A
SWATH Ships

The seaway loadings on small waterplane area twin hull (SWATH) ships are significantly different from conventional monohulls, and new design criteria are required. A series of studies was undertaken at NSWCCD during the 1970s and 1980s. As a result of those studies, a simple design algorithm for predicting the maximum lifetime side load as a function of displacement, draft, and strut length was developed (Sikora, Dinsenbacher, and Beach 1983). The side load algorithm was based on open ocean operations of ships in the 3,000 LTon to 30,000 LTon sizes. An alternative algorithm that extends the bounds of applicability down to vessels as small as 50 LTons was presented by Sikora (1995).

Algorithms are also presented for predicting slam pressure distributions and magnitudes for SWATH ships in the 50- to 30,000-LTon range. The algorithms are functions of the length of the cross-structure and include factors for modifying the pressure magnitudes as functions of the size of the applied patch (i.e. pressure/area functions). Both the primary and slam pressure algorithms have since been incorporated into the American Bureau of Shipping (ABS) rules for SWATH ships.

SWATH Ship Characteristics

Table A-1 presents the ship characteristics for the SWATHs that were used to develop the transverse side force (Shear force, TSF) algorithm.

Table A-1. SWATH Ship Particulars*

Ship	Displacement (LTons)	Beam**	Draft	Strut Length	Hull Length	Hull Diameter
SWATH-A	3,046	5.03	1.88	10.92	15.96	1.11
T-AGOS 19	3,500	5.27	1.63	12.52	15.31	1.35
SWATH IV-N	4,000	4.74	1.75	14.32	18.16	1.14
SWATH IV-T	4,000	4.74	2.04	14.32	18.16	1.14
CVA-N	101,000	6.00	1.50	16.15	18.27	0.84
CVA-S	101,000	4.92	1.50	16.15	18.85	0.84

* Ships are single strut per side; lengths are normalized by the cube root of displacement (Feet/LTon$^{1/3}$)

** Distance between centerlines of lower hulls

Table A-2 presents the ship characteristics for the SWATHs that were used to develop the slam pressure algorithm.

Table A-2. SWATH Ship Particulars for Slamming*

Ship	Displacement (LTons)	Wet Deck Clearance	Length of Cross-Structure
Halcyon	57	1.43	14.1
Frederick Creed	73	1.39	14.4
SSP Kaimalino	190	0.78	12.2
TAGOS 19	3500	0.70	12.5
TAGOS 23	5400	0.77	13.1

* Length dimensions normalized by cube root of displacement (Feet/LTon$^{1/3}$)

Primary Loads

The primary seaway loads acting on SWATH ships alternatively bend the struts/lower hulls inboard toward the ship centerline and then outboard. The transverse shear forces (TSF) causing this behavior can be treated as a line load on the lower hulls acting at the mid-draft depth. The following is the algorithm for predicting maximum lifetime sideloads for SWATH ships in the 50 to 30,000 LTon size range. The units of displacement are LTons and the lengths are in normalized units (feet divided by the cube root of displacement in LTons).

$$F = DTL\Delta$$

where

F = Maximum lifetime side load (LTons)

Δ = Displacement (LTons)

D = Size factor

= 4.474 - 0.913*Log(Δ) for ships between 50 and 2,400 LTons

= 1.55 - 0.75*tanh(Δ/11,000) for ships between 2,400 and 30,000 LTons

L = Length factor

= 0.75 + 0.35*tanh(0.5*Ls - 6)

where

Ls = strut length (Feet/LTon$^{1/3}$)

(for tandem strut vessels, Ls is the sum of the forward and aft strut lengths)

T = Draft factor

= 0.5319*draft (Feet/LTon$^{1/3}$)

Secondary Loads

Secondary loads consist of live loads (the weight of equipment, cargo, stores, etc.), dead loads (the weight of the structure itself), hydrostatic pressures (from stillwater, wave passing, pitching, and rolling), and slam impact pressures. The first three of these loads can be calculated

for SWATH ships in the same manner as for conventional monohull ships. The following algorithms presents a method for predicting the slam impact pressures on SWATH ships.

Slam pressures were measured during sea trials on four SWATH ships (T-AGOS 19, SSP *Kaimalino*, *Halcyon*, and the *Frederick Creed*) and two models (T-AGOS 19 and 23). Slamming loads were found to occur in head seas when the primary loads are negligible and in quartering to beam seas when the transverse bending loads are significant.

The maximum measured slam pressures were converted to equivalent pressures acting over one square meter (10 square feet). Next, maximum lifetime slam pressures (psi) were calculated using the following equation which is based on the ratio of the Weibull function for maximum measured to maximum lifetime values:

$$Pmax = Pmeas*(Ln\ N_{life}/Ln\ N_{trials})^{2/3}$$

where N_{trials} is the number of slamming events during the time at sea when slamming occurred, and N_{life} is the number of slamming events during the life of the ship:

$$N_{trials} = \text{slam rate}*\text{time at sea.}$$

$$N_{life} = \text{lifetime at sea} * \text{slam rate} * \text{percentage of time when slamming can occur}$$

A lifetime of 5400 days (30 years * 288 days at sea per year * 0.625 for the five beam through head seas operations out of eight possible headings) at sea was assumed with a slam rate of 10 slams per hour. Again, higher slam rates occurred in the conditions of extreme slamming, but when all of the conditions were lumped together, an average slam rate of 10 slams per hour was recorded. The slam pressures from the ships in the database were Froude scaled to ships in the 50-LTon to 30,000-LTon range, converted to patch loads over one square meter, and extrapolated to maximum lifetime pressures.

The maximum lifetime slam pressures were found to be independent of the wet deck clearance. The average of the maximum pressure (in units of psi) of the ships in the database (on the forward portion of the wet deck) was found to be approximately equal to the length of the box or cross-structure (in units of meters) for ships throughout the range (50 to 30,000 LTons). However, for design purposes it is suggested that the more conservative upper limit of the values in the database be used. The following algorithm predicts the design slam pressures for SWATH ships:

$$Pmax\ (psi) = Lf * Lb^{1.08}$$

$$Pmax\ (kPa) = 6.9 * Lf * Lb^{1.08}$$

where Lb is the box length in units of meters. The factor Lf is the longitudinal distribution of pressure as found in Figure A-1. The transverse and vertical extents the slam pressures are applied over are shown in Figure A-2. The pressures predicted by this algorithm are applied as static equivalent pressures over a one square meter (10 square foot) patch.

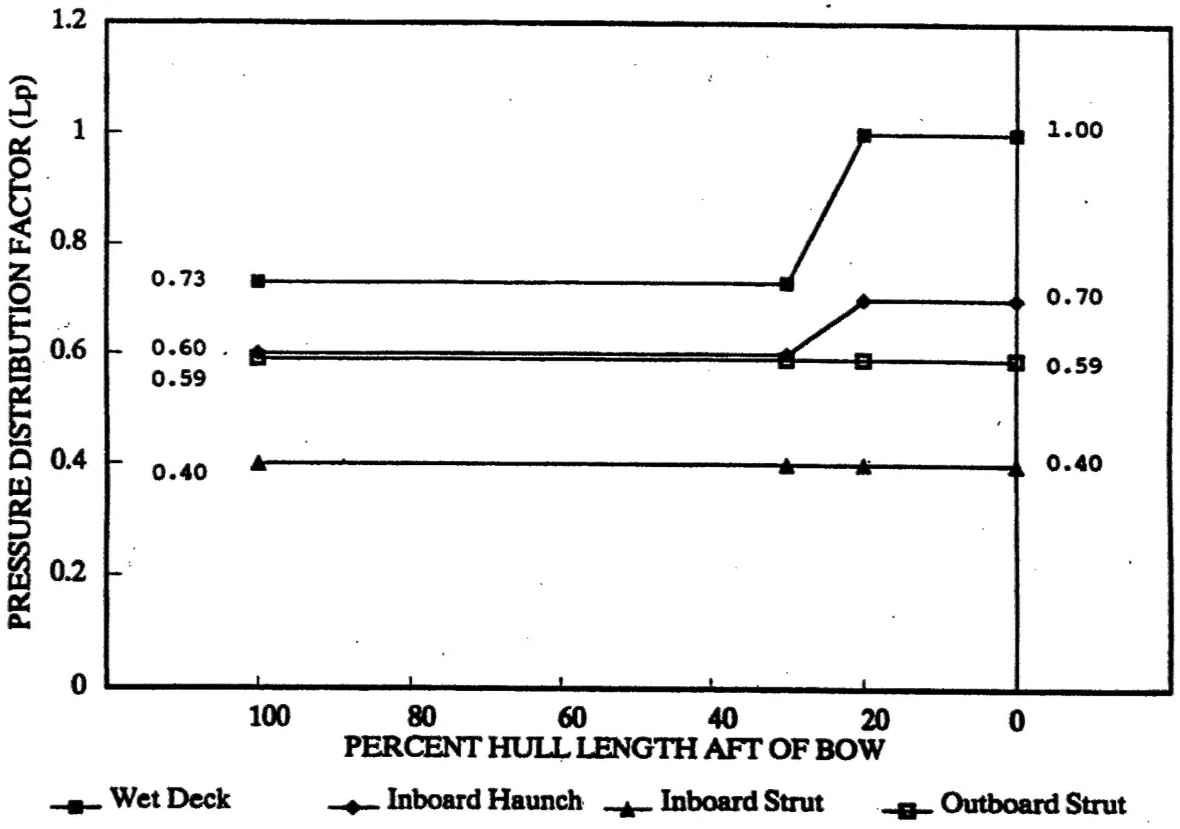

Figure A-1. Longitudinal Distribution of Slam Pressures on SWATH Ships

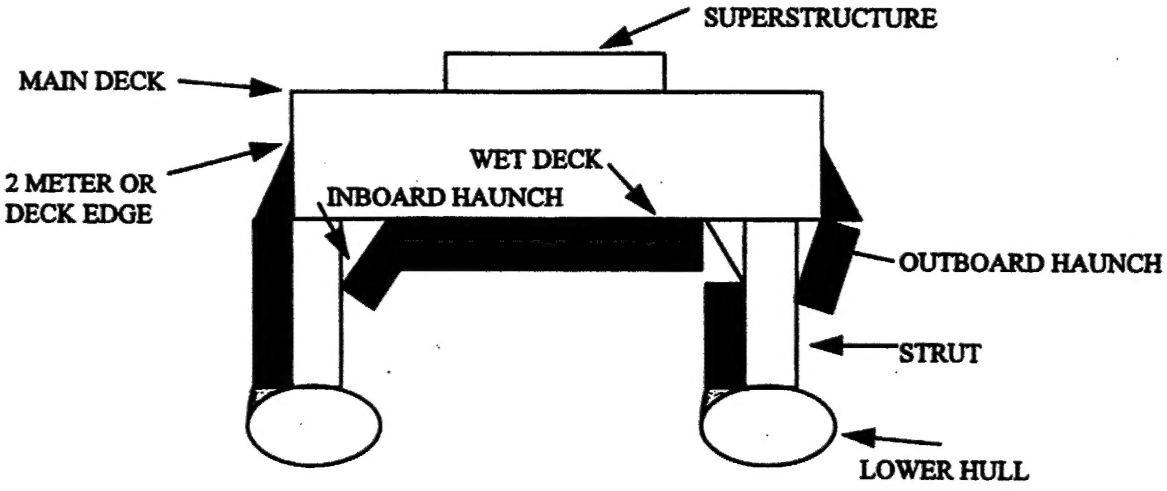

Figure A-2. Transverse Distribution of Slam Pressures on SWATH Ships

These design algorithms are for open ocean, unrestricted operations. If a given vessel is to be restricted to protected waters, a reduced number of lifetime slam events can be used in Equation (2). The number of slam events for N_{trials} and the maximum measured pressures can be obtained by Froude scaling the data in Sikora (1995) to the corresponding ship size.

In order to convert the above slam pressures to design pressures (Pdesign) for other panel sizes, the following algorithm is presented:

$$Pdesign = Pmax * Kd / Kn$$

where Kn corresponds to the nominal panel area (A = 1 m^2 [10 ft^2]) and Kd corresponds to the design area (A = desired panel size). Both Kd and Kn are the pressure/area reduction factors described in reference 7. Algorithms were fit to the curves:

$$Kn \text{ or } Kd = 1.0 \qquad \text{for } A/Ar < 0.00025$$

$$= 0.2776 + 0.0154 * (- \log_{10}[A/Ar])^3 \qquad \text{for } 0.00025 < A/Ar < 0.226$$

$$= 0.09 + 0.37 * (- \log_{10}[A/Ar])^{1.5} \qquad \text{for } 0.226 < A/Ar < 1.0$$

where A = panel area

Ar = reference area = 0.06 * Lb * B

Lb = length of box or cross-structure

B = total ship breadth, shell to shell

note: A and Ar must be in consistent units.